# PTYS 594a

# Planetary Field Geology Practicum

# Nov. 21-23,1992

# White Sands, New Mexico

APPROXIMATE ITINERARY

Saturday, 21 November:

8:30 am Distribute handouts, Depart Hawthorne house, drive E on Broadway blvd.
9:00 am Turn S. on Freeman. Observe geology of Rincon mts. --L. McFarlane and S. Engel. Continue S. to I-10, via Houton rd. then E. on I-10
10:00 am Exit I-10 at Pantano. Stop at Cross Hill Quarry: Pantano Formation and landslide --C. Steffens
Continue E. on I-10. Jim Head will describe the San Pedro Valley fossils.
11:30 am Stop at Texas Canyon rest area. Fractures and weathering of granite plutons -- V. Hillgren. Continue E. on I-10.
12:00 noon Exit I-10 at exit 331, follow Route 666 3 miles S. to Cochise overpass and RR track on Willcox Playa. Discuss geology of Willcox Playa--J. Pedicino. Continue along dirt road parallel to RR tracks (state of playa permitting).
1:00 pm Lunch on Willcox Playa.
2:00 pm Stop on E. side of playa, observe and discuss clay dunes--B. Bottke. Continue S. on Rte. 186 to Chiricahua National Monument.
2:30 pm Drive over sumit of Chiricahuas, make several stops to observe welded tuffs--E. Howell and M. Nolan. Hike to overlook near summit of mountains.
6:30 pm Camp on E. Side of Chiricahuas. **Temperatures may go down into the 30's, so bring a warm sleeping bag or blankets and appropriate clothing!**

Sunday, 22 November:

8:00 am Break Camp, drive N on rte 80, turn E. on I-10
9:30 am Arrive Rockhound State Park near Deming, NM. Discuss geology of NM, Low-angle subduction model of SW geology--A. Rivkin, J. Stansberry.
10:30 am Continue E. on I-10, pass through Las Cruces on I-70, stop outside Organ. Discuss geology of Rio Grande Rift --J. Johnson.
11:30 am Continue E on I-70, to White Sands National Monument. Stop at Monument, short hike in dunes. Discuss history of dunes, aeolian processes in general--A. Asphaug and J. Grier.
12:30 pm Lunch at White Sands NM, more discussion of eolian transport, Earth and Mars.
2:00 pm Continue N on I-70 toward Alamogordo, N on Rte. 54 to Carizozo. Proceed W. on Rte 380.
3:30pm Arrive Valley of Fires state park. Discuss Carizozo lava flow, pahoehoe emplacment processes, lava tube formation--M. Lemmon and G. Komatsu.
4:30 pm Continue W. on Rte. 380 toward Socorro.
6:00 pm Camp at low elevation in Rio Grande Rift in vicinity of Socorro.

Monday, 23 November:

8:00 am Break Camp, drive W on Rte. 60.
9:00 am Arrive VLA (Very Large Array radio interferometer), stop, tour facility.
11:30 am Depart VLA, continue W. on Rte. 60 to Datil, then S on Rte 12.
12:30 pm Lunch stop in Gila National Forest
1:30 pm continue S. on Rte. 12 to Rte 180, S on 180 to Silver City. Continue on Rte. 90 S. to Lordsburg, then W. on I-10 to Tucson
6:00 pm (with luck) arrive Tucson, unpack vans, go home.

# Proposed Route

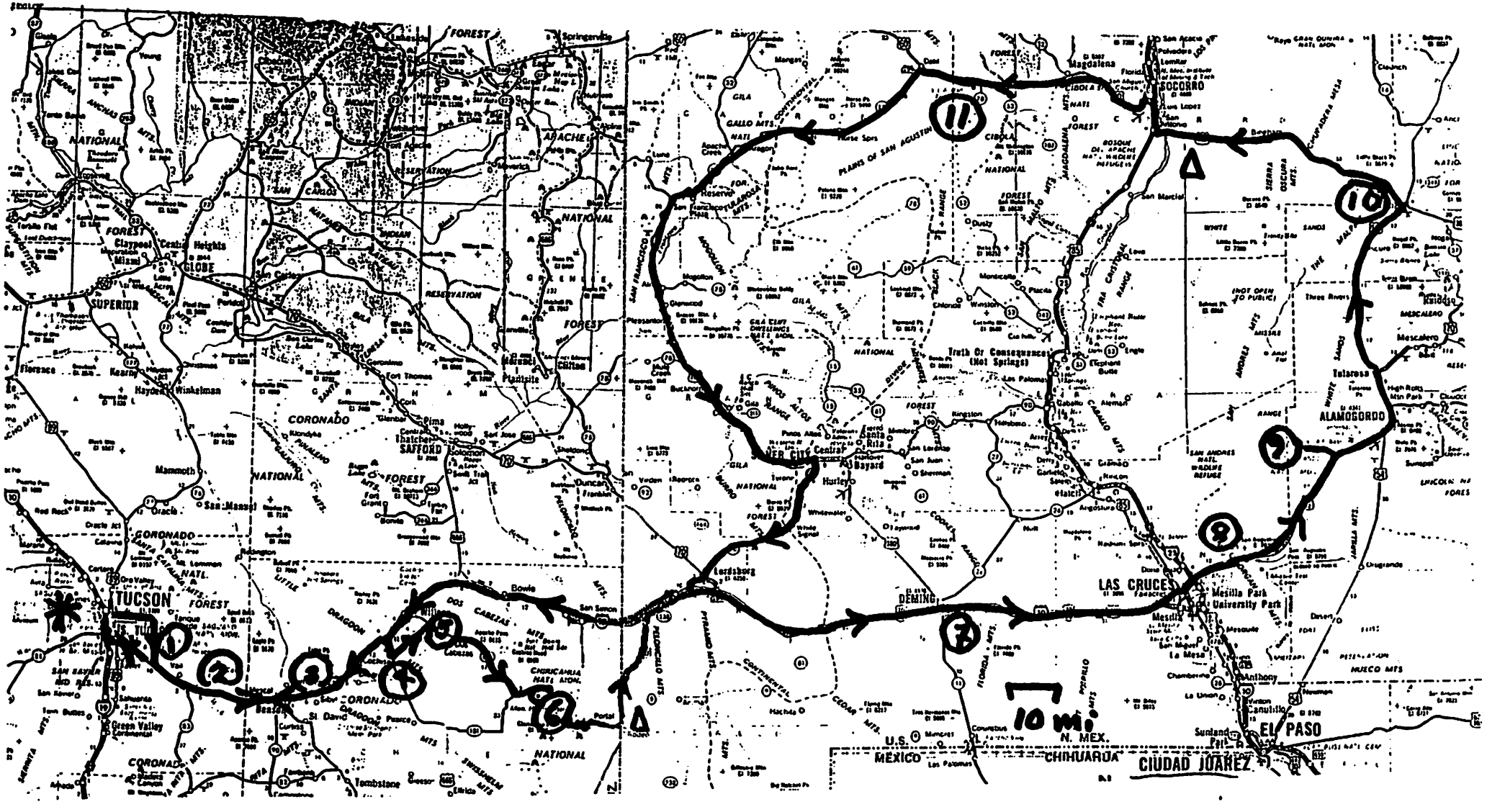

GENERAL GEOLOGIC TIME SCALE

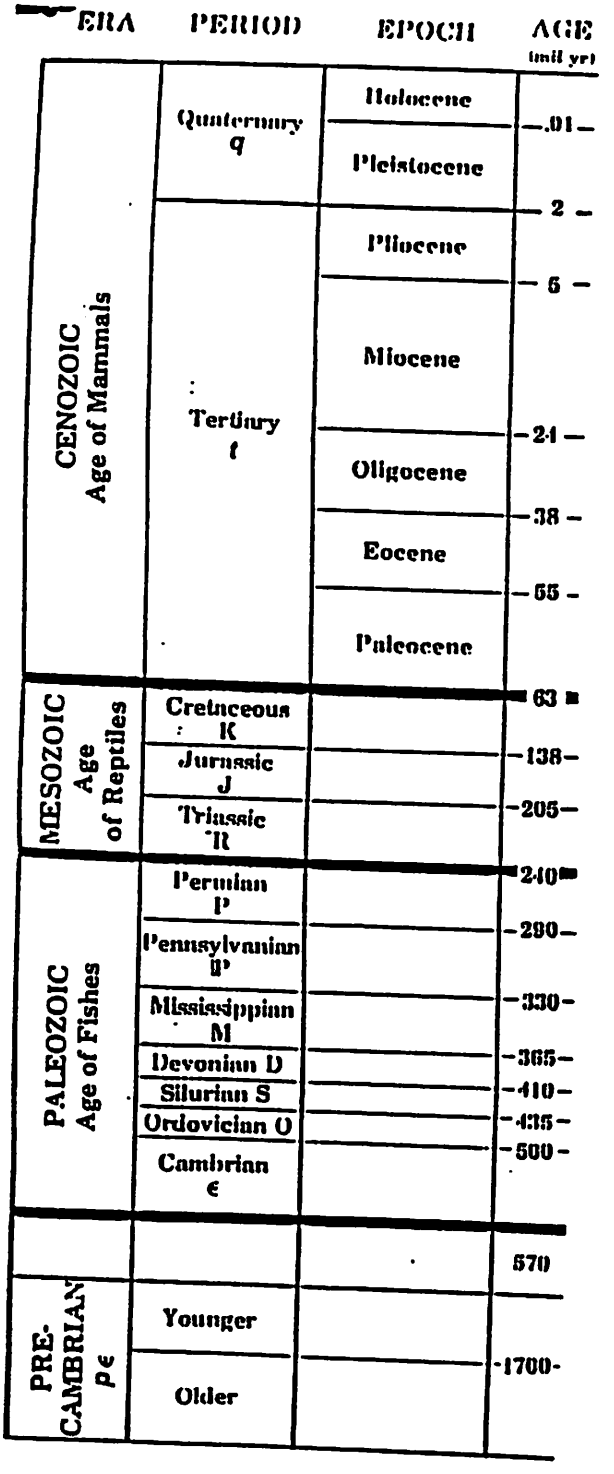

# Day 1:

# Tucson to the Chiricahuas

# Metamorphic Core Complexes

## (Tortolitas, Santa Catalinas, Rincons)

By Lisa McFarlane and Steffi Engel

**Core rocks:**

- granite with gneissic texture
- lesser amounts of Pinal Schist intruded by granitic rocks

**Cover rocks:**

- sedimentary and metasedimentary rocks
- granitic rocks without gneissic texture

**Gravel deposits:**

- conglomerates

**Precambrium (1.6 b.y.)**

- clastic deposition (Pinal Schist), uplift + erosion,
- clastic deposition (Apache group) more uplift + erosion,

**Paleozoic-Cenozoic (570-0 m.y.)**

- marine transgressions, sediments, limestone

**Mesozoic (240-63 m.y.)**

- start of volcanic activities (ryolithic tuffs)

**Cenozoic**

- major volcanic activities
25 m.y. - plutonic emplacement and metamorphism ended
15-8 m.y. - Basin and Range began to form
Holocene - gravel deposits derived from the mountains deposited in basins

A *caldera* is a volcano that has subsided into a round or oval depression, much as an apple pie crust, inflated by steam during baking, might collapse into the hollow below it once the pie cools

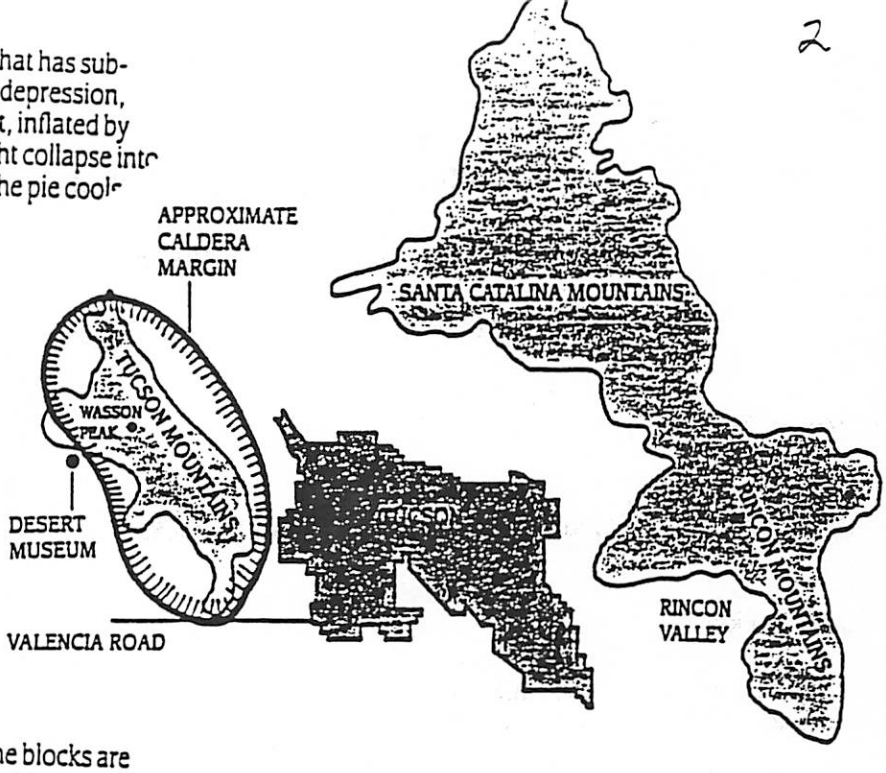


*Map of Tucson area, showing caldera outline.*

Tucson Mountain Chaos, the blocks are now known as megabreccia blocks. Most of the rocks visible from the Pass are rhyolite tuff, but the Pass itself is cut into a giant megabreccia block of sandstone that fell into the pit and was sealed in rhyolite ash.

---

metamorphic core complexes. The lowest layers of these complexes are granitic rocks, and these are overlaid by a thick blanket of metamorphosed granites that appear stretched. Brittle upper volcanic and sedimentary layers were balanced on top of the rising complex. These layers have often slid slowly into nearby areas, breaking and tilting as they moved horizontally and downward in response to gravity.

The Santa Catalina Mountains are a metamorphic core complex. The granites at the bottom of the complex are exposed by erosion in many areas near the top of the mountains. The metamorphic layers are called the Catalina Gneiss. This formation is well exposed from Pusch Ridge to Sabino Canyon and beyond. The age of metamorphism of these rocks is about 17 to 30 million years (Mid-Tertiary time).

*Metamorphic core complex and detachment fault.*

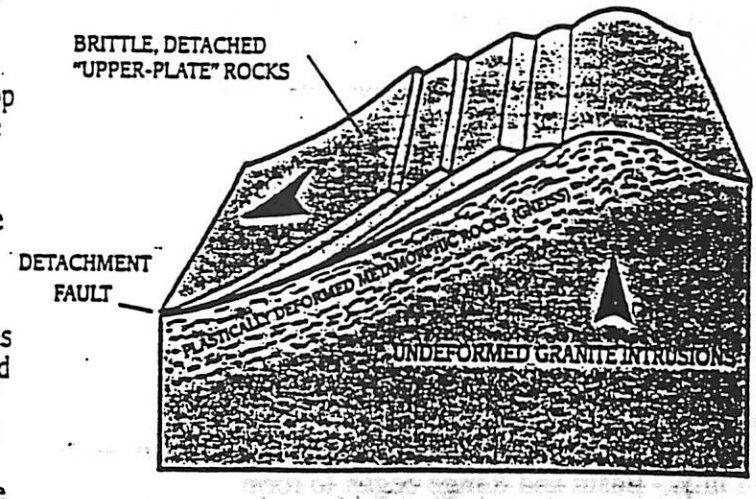


During extension, the brittle upper "magazine" rocks would often separate from the lower layers and travel considerable distances horizontally.

Plutonic and metamorphic core rocks range in age from early Proterozoic to mid-Tertiary, and form nearly contiguous exposures that occupy much of the Tortolita, Santa Catalina, and Rincon mountains

(Wernicke and Burchfiel, 1982), has influenced the evolution of continental crust through time as surely as has the contractional strain of orogeny. The dozens of Cordilleran metamorphic core complexes distributed along some 2,500 km of the intermountain belt from southern Canada to northern Mexico (Coney, 1980b) are worthy of careful study because they constitute perhaps the most dramatic record of intraplate extension exposed

## CRUSTAL EXTENSION

Middle Tertiary tectonic activity in Arizona was dominated by widespread normal faulting and fault-block rotation that accommodated major northeast-southwest to east-northeast—west-southwest crustal extension. Movement occurred on low- to high-angle normal faults, and many high-angle normal faults are known or suspected to be truncated downward by, or to flatten downward and merge with, major detachment faults. Detachment faults in Arizona and the southwest have several to several tens of kilometers of displacement and are the most important structural features of mid-Tertiary age in the Basin and Range Province.

### Causes of Extension

The ultimate cause of mid-Tertiary magmatism and extension is controversial. Magmatism has generally been considered to have resulted from subduction of oceanic lithosphere beneath western North America, and space-time patterns of magmatism have been viewed as the result of the changing dip and configuration of the subducted lithosphere

70 MILLION YEARS AGO

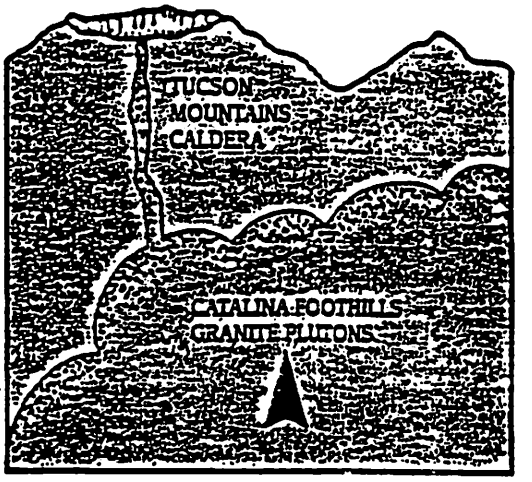


The proposed reason for regional extension is that a large amount of hot, mushy magma had intruded into the base of our area. The intrusions heated and distended the region, causing the rocks to arch upwards. Then, as the buried mush relaxed and spread out, the brittle overlying rocks were pulled apart or extended.

30 to 17 MILLION YEARS AGO

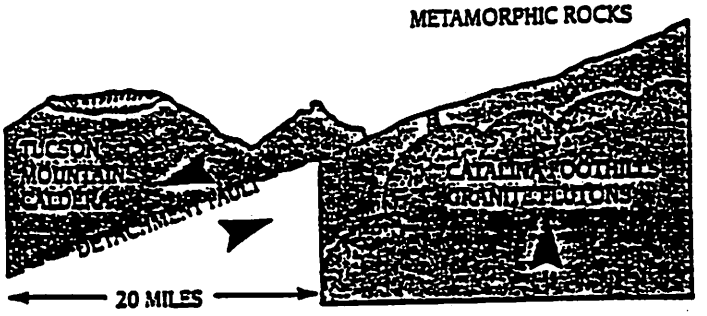


One line of evidence for substantial stretching comes from rocks of the Rincon Mountains, an extension of the Catalinas. Matching rocks were found 20 miles apart, showing that slippage here was of that magnitude. The eastern rocks were on the bottom "magazine" and the western ones, in Rincon Valley, were on the top, but displaced 20 miles.

PRESENT TIME, AFTER TUCSON BASIN SUBSIDES AND EROSION OCCURS

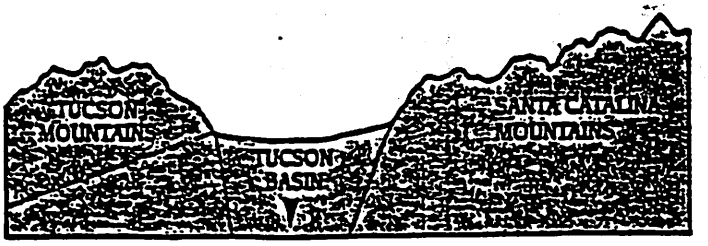


Other evidence is derived from a comparison of certain rocks of the Catalinas with those of the Tucson Mountains. The rocks in question are at the same elevation, frowning at each other across the Tucson Basin. Yet the mineralogical character of the Catalina rocks shows that they were formed perhaps eight miles deep in the crust, while the Tucson Mountain rocks were formed at the surface. Therefore, the Catalina rocks must have been uplifted eight miles to their present position.

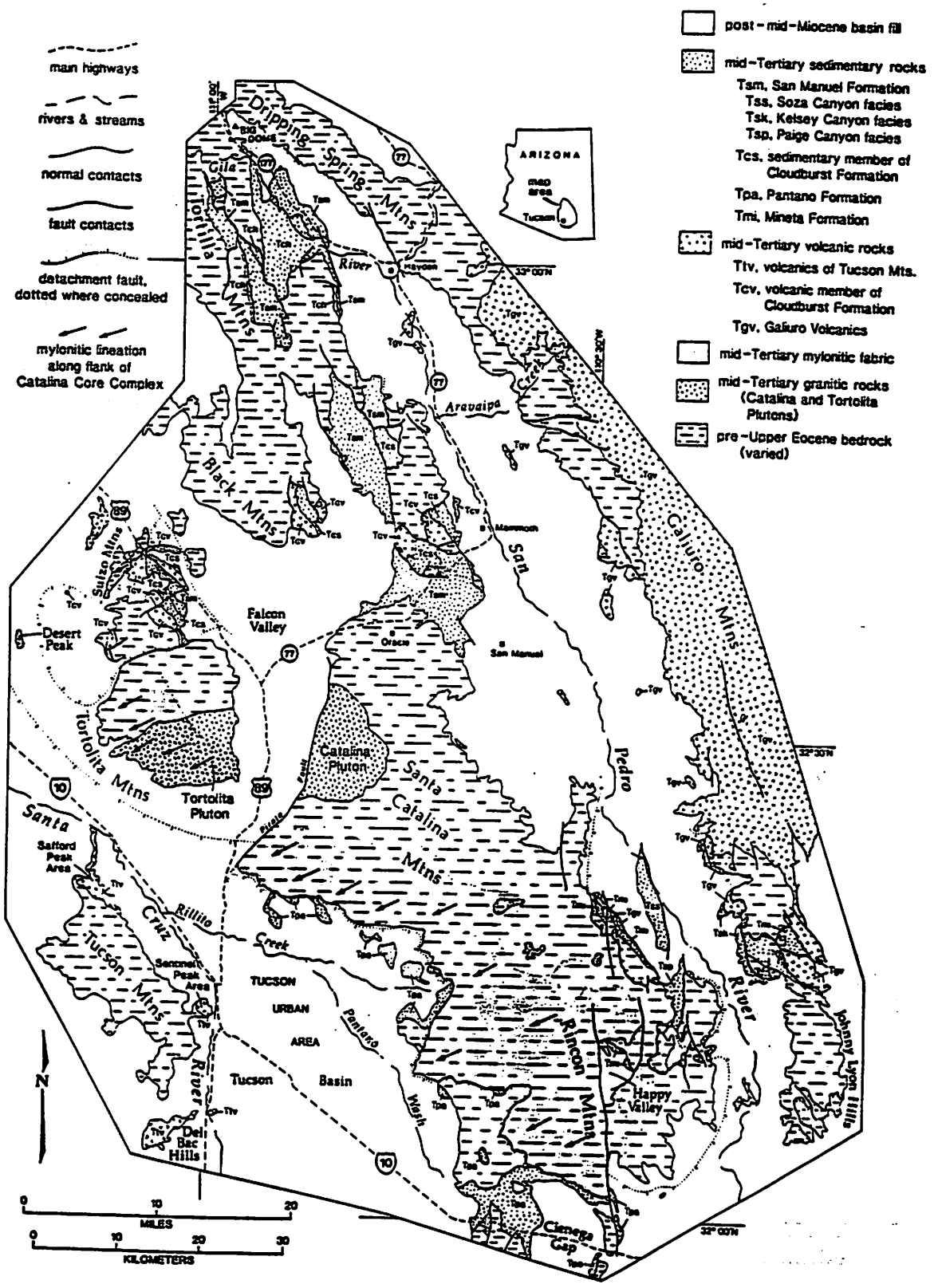


Figure 2. Geologic sketch map of Catalina core complex (mylonitic foliation and lineation along southwest flank) and San Pedro trough (traversed by San Pedro River and by Gila River below their confluence) showing areal distribution of tilted homoclines of mid-Tertiary volcanic and sedimentary successions in relation to exposures of older bedrock and younger basin fill; modified after Dickinson and Shafiqullah (1989).

(greater than sand size, or 2 mm in diameter), angular, and broken rock fragments that are cemented together in a finer-grained matrix (which may or may not be similar to the larger fragments) and that can be of any composition, origin, or mode of accumulation; the consolidated equivalent of rubble. According to Woodford (1925, p.183), the rubble content must be greater than 80%. Breccia is similar to *conglomerate* except that most of the fragments have sharp edges and unworn corners; the term "breccia" formerly included conglomerate, and is still sometimes so used in Europe. The rock can be formed in many ways, chiefly by sedimentation (*sedimentary breccia*), igneous activity (*igneous breccia*), and diastrophism (*tectonic breccia*).

**brecciated** [geol] Converted into, characterized by, or resembling a breccia; esp. said of a rock structure marked by an accumulation of angular fragments, or of an ore texture showing mineral fragments without notable rounding.

**caldera** A large, basin-shaped volcanic depression, more or less circular or circuelike in form, the diameter of which is many times greater than that of the included vent or vents, no matter what the steepness of the walls or form of the floor (Williams, 1941). See also: *collapse caldera; erosion caldera; explosion caldera.*

**cataclasis** Rock deformation accomplished by fracture and rotation of mineral grains or aggregates without chemical reconstitution. See also: *cataclastic metamorphism; cataclastic rock.*

**cataclasite** A rock formed by cataclasis; a *cataclastic rock.*

**chlorite** (a) A group of platy, monoclinic, usually greenish minerals of general formula: $(Mg,Fe^{+2},Fe^{+3})_6AlSi_3O_{10}(OH)_8$. It is characterized by prominent ferrous iron and by the absence of calcium and alkalies; chromium and manganese may also be present. Chlorites are associated with and resemble the micas (the tabular crystals of chlorite cleave into small, thin flakes or scales that are flexible, but not elastic as those of mica), and are widely distributed, esp. in low-grade metamorphic rocks, or as alteration products of ferromagnesian minerals in igneous rocks.

**chlorite schist** A schist in which the main constituent, chlorite, imparts the schistosity by parallel arrangement of its flakes. Quartz, epidote, magnetite, and garnet are accessories; the latter two often as conspicuous porphyroblasts.

**clastic rock** (a) A consolidated sedimentary rock composed principally of broken fragments that are derived from preexisting rocks (of any origin) or from the solid products formed during chemical weathering of such rocks, and that have been transported mechanically to their places of deposition; e.g. a sandstone, conglomerate, or shale, or a limestone consisting of particles derived from a preexisting limestone. See also: *epiclastic rock.* Syn: *fragmental rock.* (b) *pyroclastic rock.* (c) *bioclastic rock.* (d) *cataclastic rock.*

**clastic sediment** A sediment formed by the accumulation of fragments derived from preexisting rocks or minerals and transported as separate particles to their places of deposition by purely mechanical agents (such as water, wind, ice, and gravity); e.g. gravel, sand, mud, clay. Cf: *detrital sediment.* Syn: *mechanical sediment.*

**collapse caldera** A type of *caldera* produced by collapse of the roof of a magma chamber due to removal of magma by voluminous pyroclastic eruptions or by subterranean withdrawal of magma. Most calderas are of this type. Cf. *erosion caldera; explosion caldera.*

tion, resulting in independent styles of deformation in the rocks above and below. It is associated with folding and with overthrusting, but it is merely a descriptive term. Etymol: French, "unsticking, detachment". Cf: *tectonic denudation; disharmonic folding.* See also: *bedding-plane slip.* Syn: *detachment.* Obsolete syn: *strip thrust.*

**detachment [fault]** *décollement.*

**gneiss** A foliated rock formed by regional metamorphism in which bands or lenticles of granular minerals alternate with bands and lenticles in which minerals having flaky or elongate prismatic habits predominate. Generally less than 50% of the minerals show preferred parallel orientation. Although a gneiss is commonly feldspar- and quartz-rich, the mineral composition is not an essential factor in its definition (American usage). Varieties are distinguished by texture (e.g. augen gneiss), characteristic minerals (e.g. hornblende gneiss), or general composition and/or origins (e.g. granite gneiss). See also: *gneissic; gneissoid; gneissose.*

**gneissic** Pertaining to the texture or structure typical of gneisses, having foliation that is wider spaced, less marked, and often more discontinuous than that of a *schistose* texture or structure (Johannsen, 1931). Cf: *gneissoid; gneissose.*

**gneissic structure** In a metamorphic rock, commonly *gneiss*, the coarse, textural lineation or banding of the constituent minerals into alternating silicic and mafic layers. Syn: *gneissosity; gneissose structure.* Cf: *primary gneissic banding.*

**megabreccia** (a) A term used by Lances (1945) for a rock produced by brecciation on a very large scale, containing blocks that are randomly oriented and invariably inclined at angles from 6° to 25° and that range from a meter to more than 100 m in horizontal dimension. (b) A term used by Longwell (1951) for a coarse breccia containing individual blocks as much as 400 m long, developed downslope from large thrusts by gravitational sliding. It is partly tectonic and partly sedimentary in origin, containing blocks that are shattered but little rotated.—Cf: *chaos.*

**microbreccia** (a) A poorly sorted sandstone containing relatively large and sharply angular particles of sand set in a very fine silty or clayey matrix; e.g. a graywacke. It is somewhat less micaceous than a siltstone. (b) A breccia within fragments of a coarser breccia (Sander, 1951, p.28).

**mylonite** As introduced by Lapworth in 1885, a compact, chertlike rock without cleavage, but with a streaky or banded structure, produced by the extreme granulation and shearing of rocks which have been pulverized and rolled during overthrusting or by action of intense dynamic metamorphism in general. Mylonite may also be described as a microbreccia with fluxion structure (Holmes, 1920). See also: *protomylonite; ultramylonite; blastomylonite.*

**mylonite gneiss** A metamorphic rock that is intermediate in character between mylonite and schist. Felsic minerals show cataclastic phenomena without much recrystallization, and often occur as augen surrounded by and alternating with schistose streaks and lenticels of recrystallized mafic minerals (Holmes, 1928, p.164).

**mylonitic structure** A structure characteristic of mylonites, produced by intense microbrecciation and shearing which gives the appearance of a flow structure. Cf: *flaser structure.*

**mylonitization** Deformation of a rock by extreme microbrecciation, due to mechanical forces applied in a definite direction, without noteworthy chemical reconstitution of granulated minerals. Characteristic features of the mylonites thus produced have a flinty, banded, or streaked appearance, and undestroyed augen and lenses of the parent rock in a granulated matrix (Schieferdecker, 1959). Also spelled: *mylonization.*

**mylonization** *mylonitization.*

orogeny Literally, the process of formation of mountains.

By present geological usage orogeny is the process by which structures within mountain areas were formed, including thrusting, folding, and faulting in the outer and higher layers, and plastic folding, metamorphism, and plutonism in the inner and deeper layers.

rhyolite A group of extrusive igneous rocks, generally porphyritic and exhibiting flow texture, with phenocrysts of quartz and alkali feldspar (esp. orthoclase) in a glassy to cryptocrystalline groundmass; also, any rock in that group; the extrusive equivalent of granite. Rhyolite grades into rhyodacite with decreasing alkali feldspar content and into trachyte with a decrease in quartz. Etymol: Greek *rhyo-*, from *rhyax*, "stream of lava". Syn: *lisarite; quartz tracnyte*. Cf: *quartz porphyry*.

schist A strongly foliated crystalline rock formed by dynamic metamorphism which can be readily split into thin flakes or slabs due to the well developed parallelism of more than 50% of the minerals present, particularly those of lamellar or elongate prismatic habit, e.g. mica, hornblende. The mineral composition is not an essential factor in its definition (American usage) unless specifically included in the rock name, e.g. quartz-muscovite schist. Varieties may also be based on general composition, e.g. calc-silicate schist, amphibolite schist, or on texture, e.g. spotted schist.

---

Evolutionary cross sections of a hypothetical detachment fault-ductile shear zone and the formation of a metamorphic core complex. (A) Detachment fault is shown as initially planar below 5 km and listric above. The detachment fault projects downward across the brittle-ductile transition to become a ductile shear zone. (B) Isostatic uplift of the lower plate due to denudation leads to arching of the footwall. Footwall rocks originally mylonitized below the brittle-ductile transition rise isostatically through the transition and are overprinted by brittle structures adjacent to the detachment fault. Syntectonic sediments fill grabens and half grabens. (C) Continued arching and uplift of the footwall result in termination of detachment-fault movement to the left of the arch and formation of a secondary breakaway to the right.

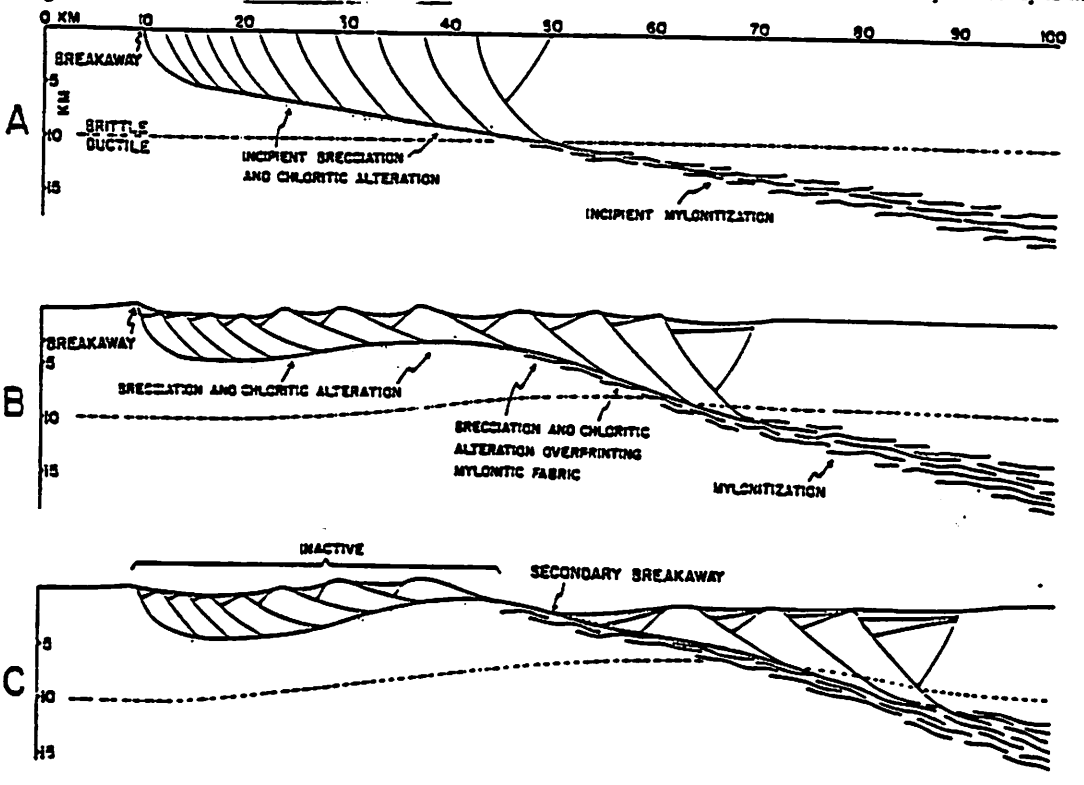


MIDDLE TERTIARY TECTONICS

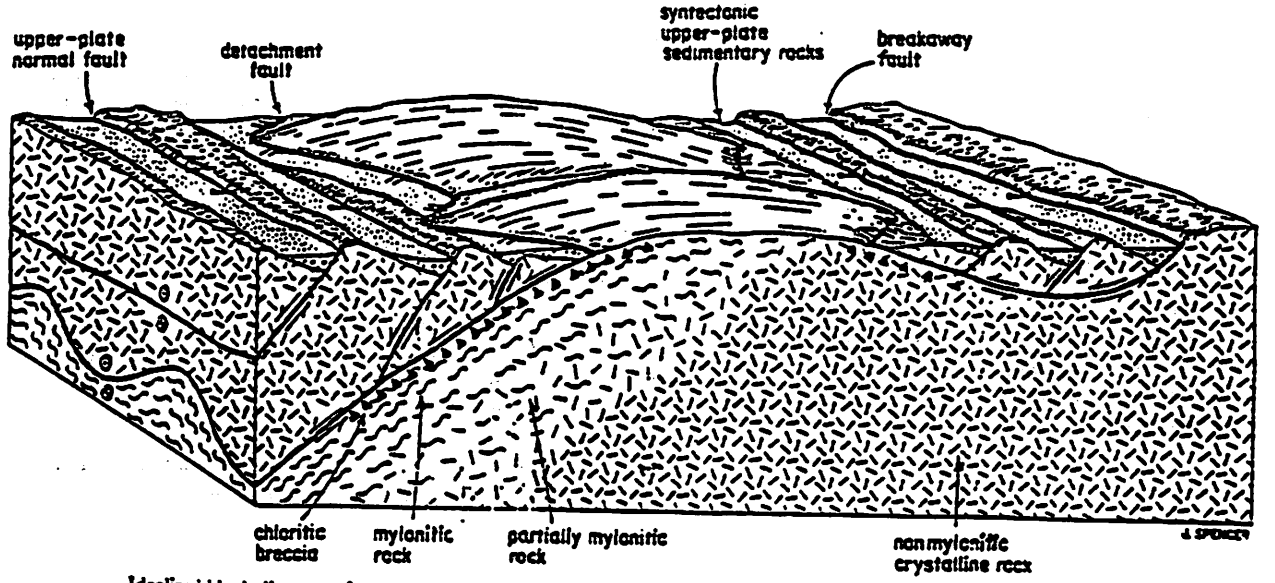


Idealized block diagram of a metamorphic core complex.

# CROSS HILL LANDSLIDE

Cathy Steffens

The base of a large landslide is exposed at the Cross Hill clay quarry in Cienega Gap. We'll look for all the features Yarnold and Lombard say we're supposed to see: deformed substrate, clastic dikes, comminuted limestone, and lots of busted up rock. The Pantano clay itself is pretty neat, too. It's mined by the Phoenix Brick Yard to make, among other things, bricks for new U of A buildings.

Landslide area: 6 $km^2$
volume: $\sim 20 \times 10^6$ $m^3$
length: 4.5 km
thickness: 1-50m in distal portion
vertical drop and horizontal travel unknown
age: sometime after deposition of Pantano ($\sim$25 Ma) and before Neogene basin fill; probably between 20-12 Ma

References:

Balcer, R.A., 1984, Stratigraphy and depositional history of the Pantano Formation (Oligocene-early Miocene), Pima County, Arizona: Tucson, U of A M.S. thesis, 107 p.

Dickinson, W.R., 1991, Tectonic setting of faulted Tertiary strata associated with the Catalina core complex in southern Arizona: GSA Special Paper 264, 106 p.

Drewes, H. , 1977, Geologic map and sections of the Rincon Valley Quadrangle, Pima County, Arizona: Tucson, USGS Map I-997.

Houser, B.B., 1992, Industrial Minerals of the Tucson Area and San Pedro Valley, southeastern Arizona: AZ Geol Survey field trip, Apr. 4-5, 1992, 55 p.

Melosh, H.J., 1987, The mechanics of large rock avalanches: GSA Reviews in Engineering Geology, vol. VII, p. 41-49.

Yarnold, J.C., and Lombard, J.P., 1989, A facies model for large rock-avalanche deposits formed in dry climates, in Colburn, Abbott, and Minch, eds., Conglomerates in basin analysis: Pacific Section, S.E.P.M. Book 62, p.9-31.

Look for these exciting features at Cross Hill:

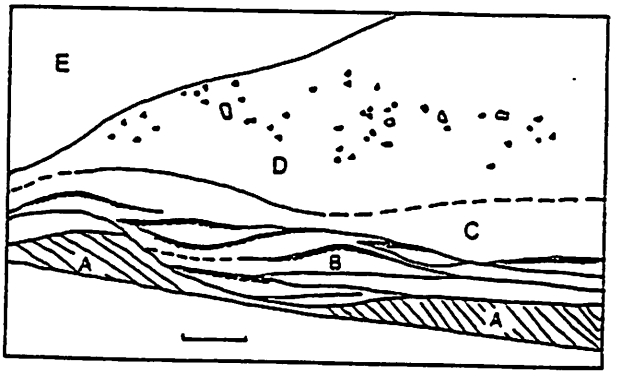


Figure 12. Basal contact of the Cross Hill breccia deposit at Cross Hill clay quarry, showing (A) east-dipping undeformed substrate sediments, (B) imbricated slices of sandstone and mudstone substrate sediments (marker bed shaded), (C) interval of thoroughly comminuted limestone, (D) matrix-rich breccia with cobbles, and (E) matrix-poor breccia. Scale bar is 1 m.

Yarnold + Lombard, 1989, p. 19.

## Distal

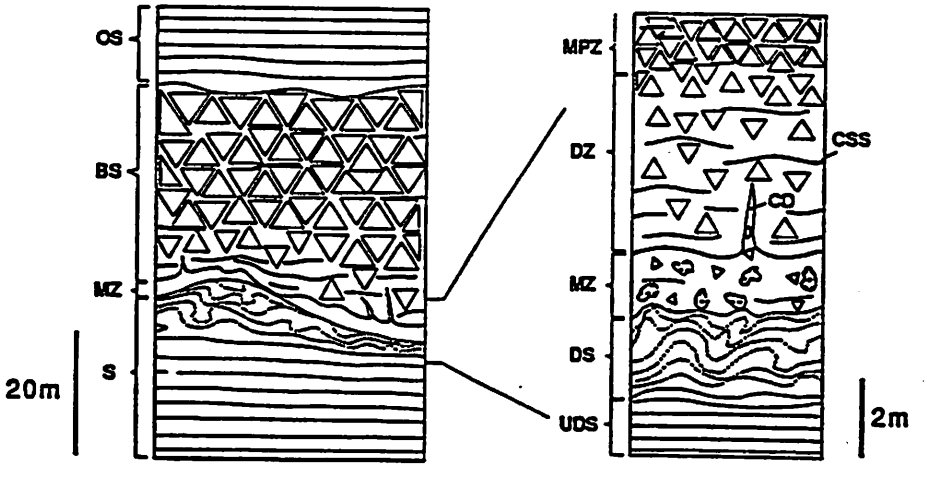


Figure 15. Characteristic features within ~~proximal and~~ distal portions of large rock-avalanche deposits investigated, showing: substrate (S); undisturbed substrate (UDS); disturbed substrate (DS); mixed zone of entrained substrate and comminuted breccia (MZ); disturbed zone (DZ) of the breccia sheet (BS) that displays comminuted slip surfaces (CSS), and is intruded by clastic dikes (CD) and intrusive stringers (IS; load structures and poorly-developed clastic dikes) derived from the mixed zone; matrix-poor zone (MPZ) of the breccia sheet; and overlying sediments (OS). In places, a discontinuous megabreccia cap occurs along the top of the breccia sheet.

Yarnold + Lombard, 1989, p. 21.

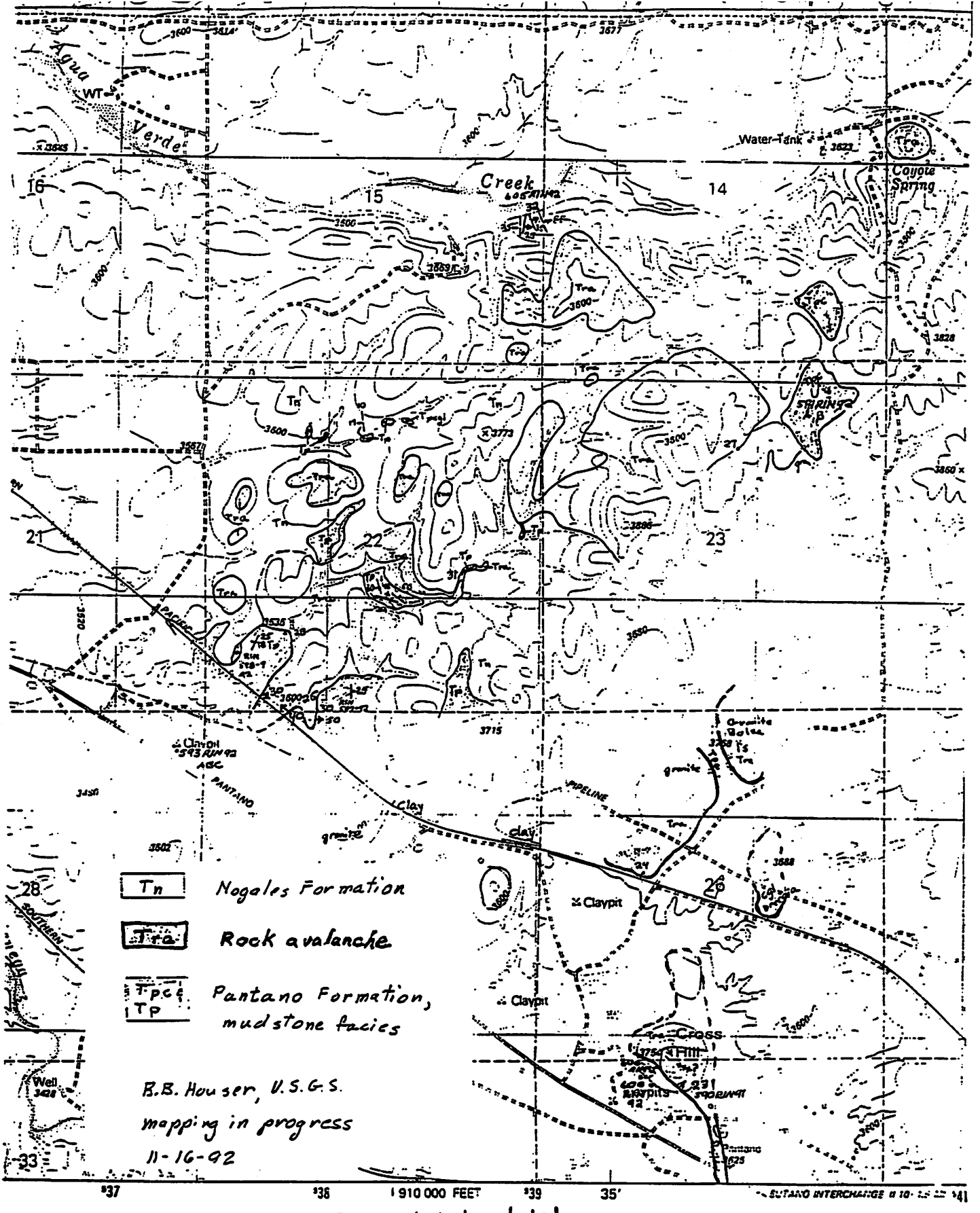


ed by the Geological Survey

thods from aerial
cked 1976

# Texas Canyon

with your charming hostess
Val "the Gal" Hillgren

The Texas Canyon Stock:

- quartz monzonite (lots of feldspar)
- dated at ≈ 50 Ma (Laramide Orogeny)
- intrudes the Hildago and Cochise thrust faults in the southern part of Little Dragoons

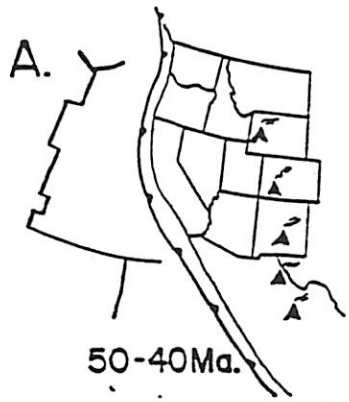


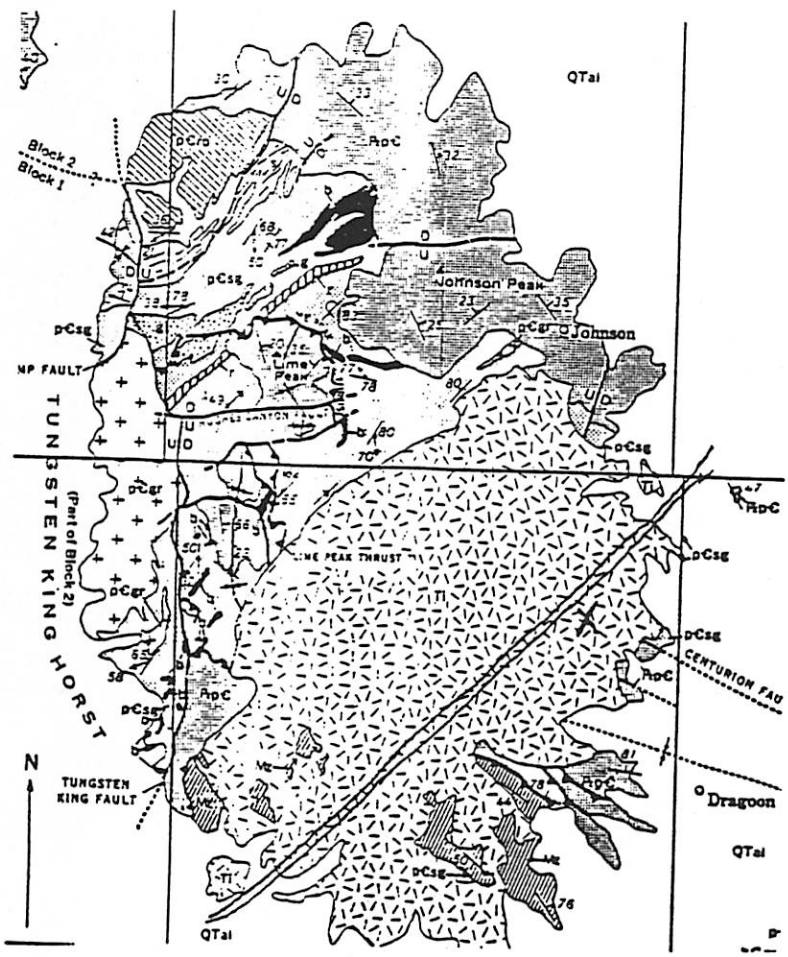


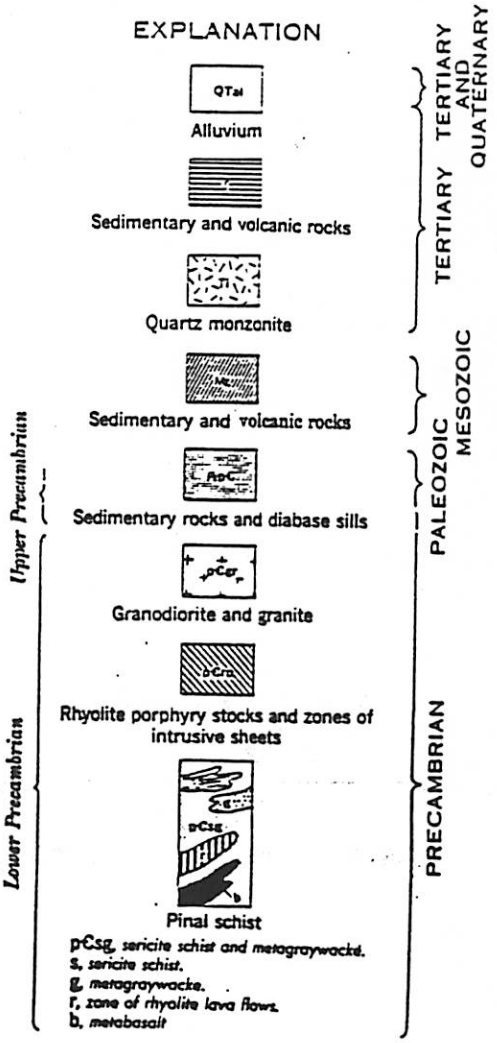

# Spheroidal Weathering

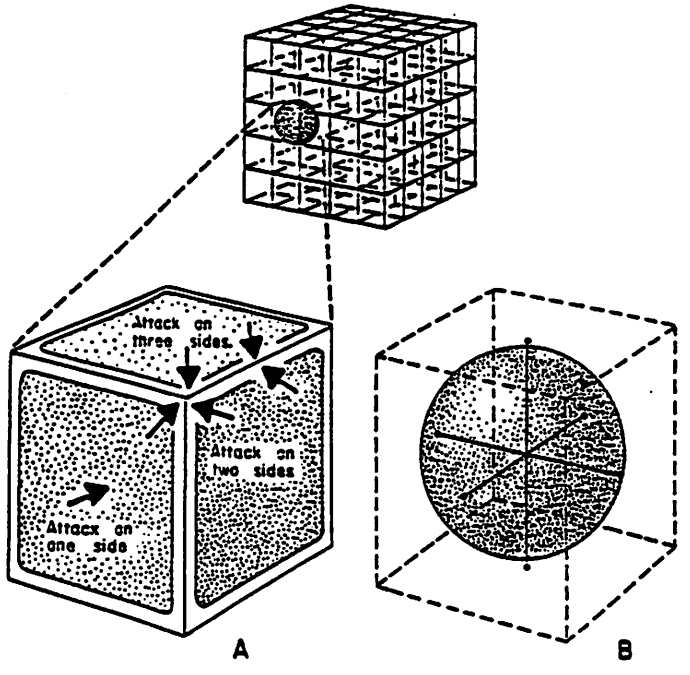


**Fig. 17.6 Geometry of spheroidal weathering.**

Kinds of Rocks that Spheroidally weather:
① have no layering
② are homogeneous
③ have lots of feldspar (usually granite-like rocks)

Why is feldspar so important?
It's strong but weathers easily:
feldspar + rainwater → clay + water with stuff dissolved in it.

Finally, need a set of joints - 3 sets of mutually ⊥ fractures.

Grus: Coarse fragments of quartz and feldspar weathered loose from the rock

And Climate helps formation of spheroidal boulders. In wet climates weathering occurs too quickly and nice soils form & allowing rocky plants and trees to obscure the boulders.

Some Examples of spheroidally ~~Spheroidally~~ oops! weathered boulders

Warning! Warning! These are NOT in Texas Canyon, but along the Benline Highway

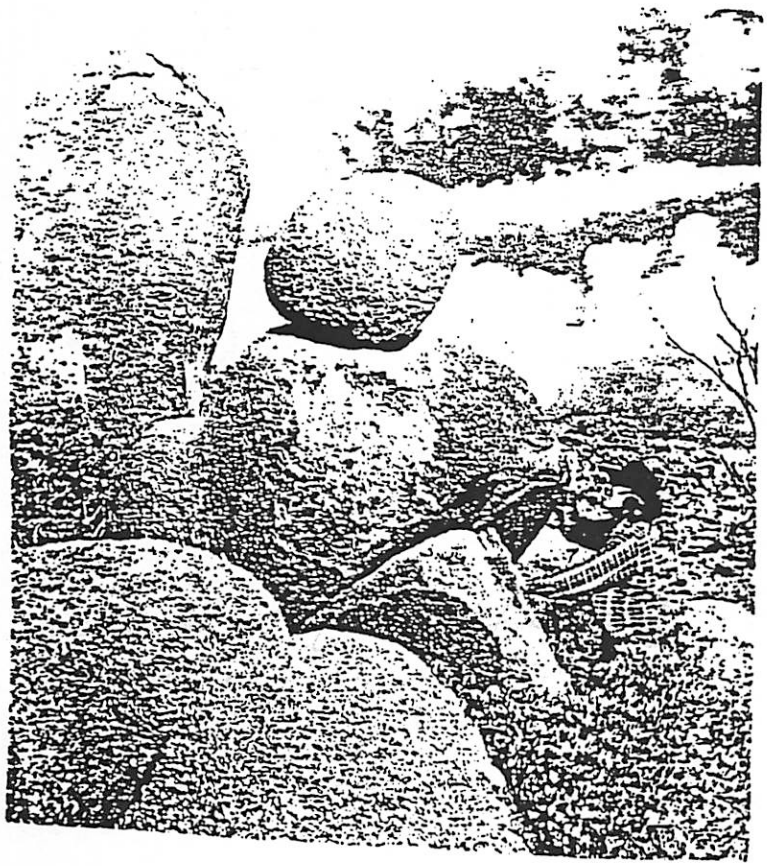

# The Geologic History of the Willcox Playa

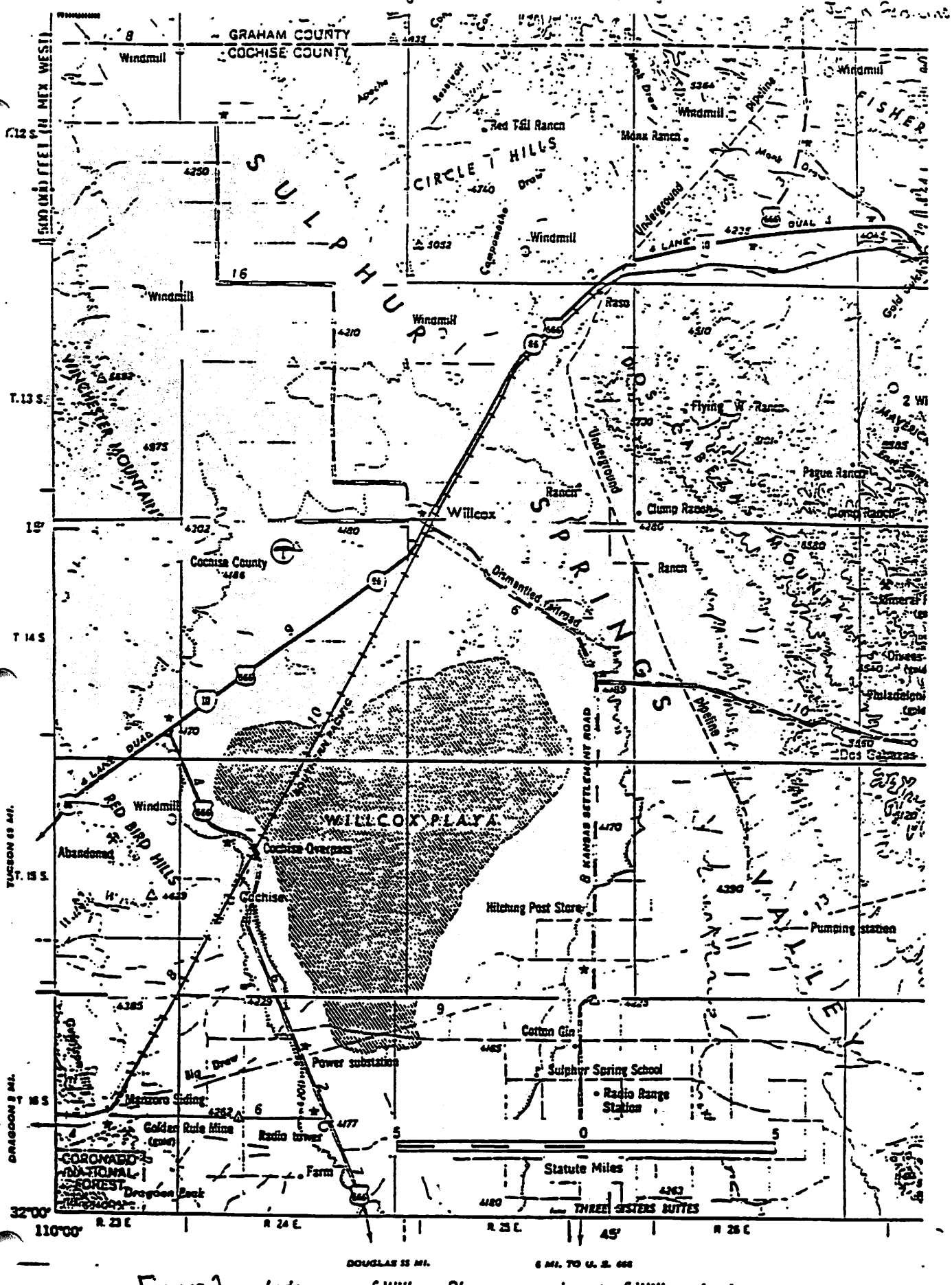


Figure 1. *Index map of Willcox Playa area and part of Willcox basin.*

From: Schreiber, J.F., Geology of Willcox Playa, N.M. Geol. Soc. Guidebook, 1978 p. 273

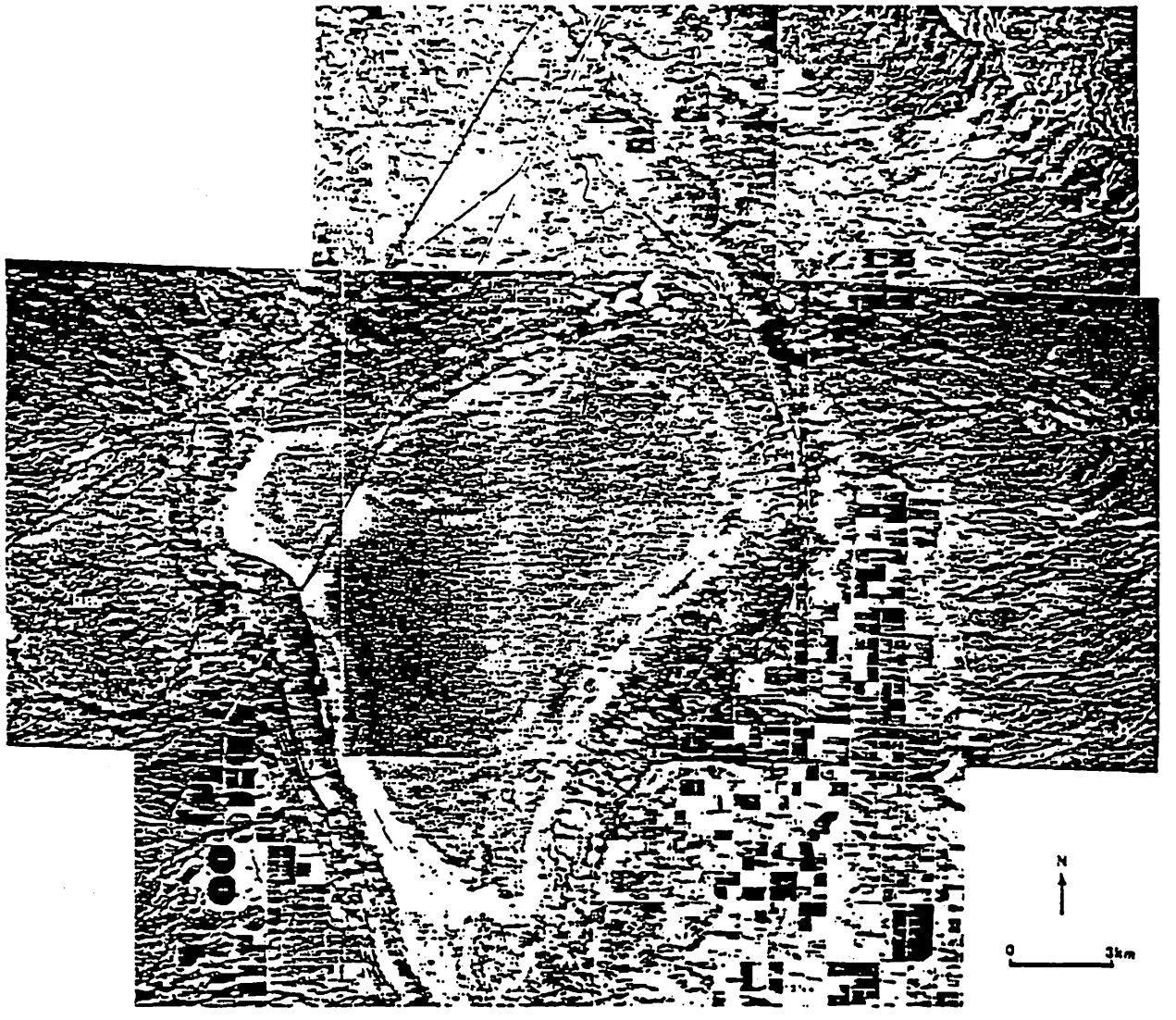


Figure 3. Aerial photo of the central portion of the Willcox basin. The 1274 m shoreline of Lake Cochise (LC), the Willcox Playa (WP), dune field (DF), bajadas (B), Dos Cabezas Mountains (DC), and Red Bird Hills (RB) are indicated.

From: Waters, M., Woosley, A., The Geoarchaeology & Prehistoric History of the Willcox Basin, SE Arizona, Journal of Field Archaeology, Vol. 17, 1990, p. 165.

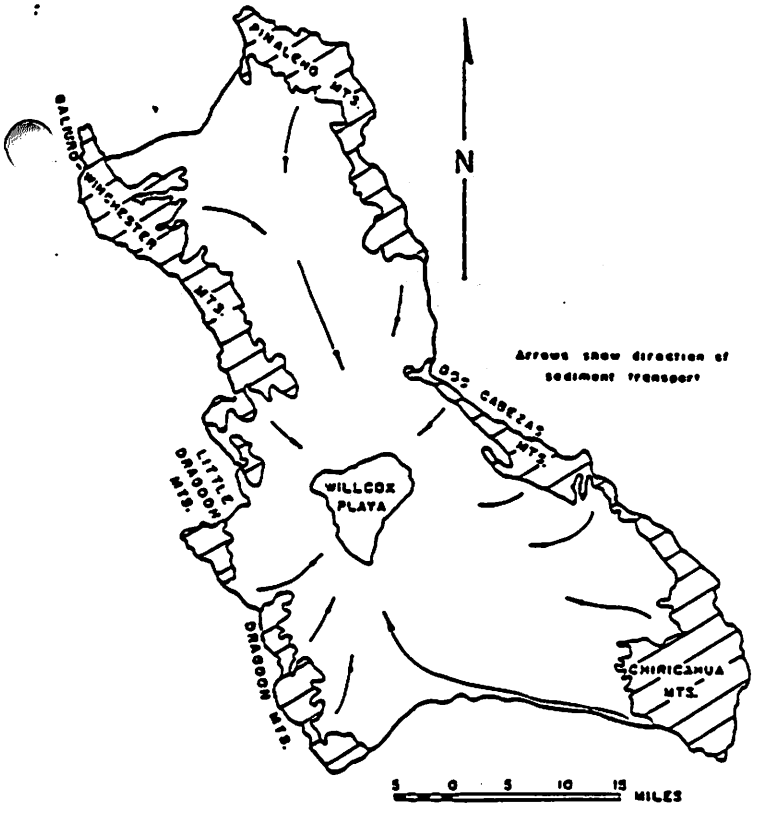


Figure 3. *Willcox basin drainage area.*

From Schreiber, J.F. p. 274

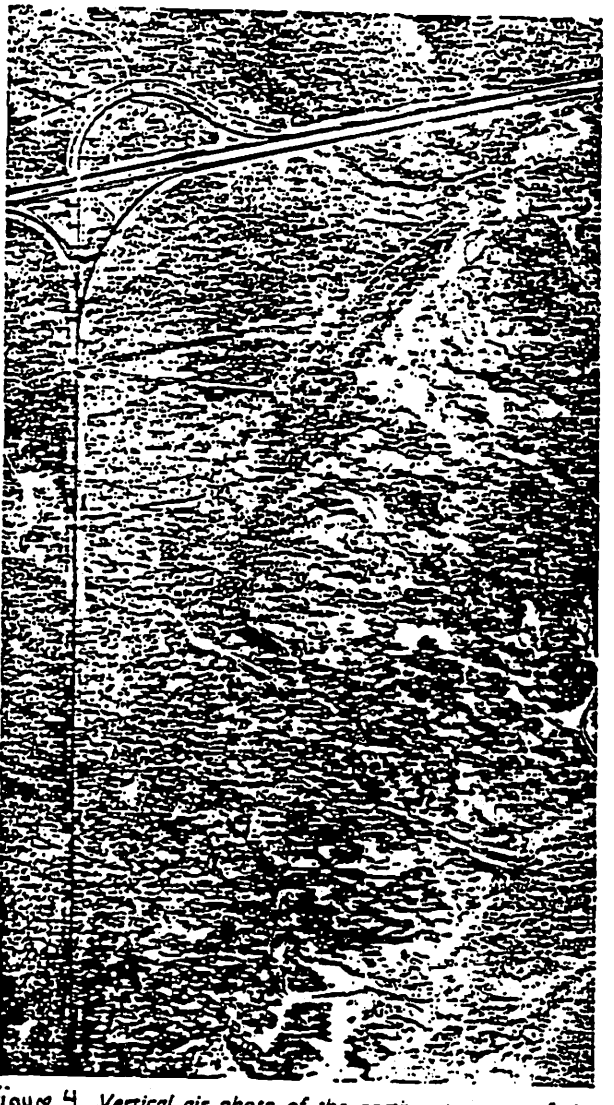

Figure 4. *Vertical air photo of the northwest corner of the playa near the Interstate 10-U.S. 666 overpass; U.S. 666 parallels the left side. The beach ridge is located by the line of dark mesquite trees that parallel U.S. 666 for a short distance before swinging to the right. Photo taken May 1, 1975 by the Arizona Department of Transportation.*

From Schreiber, J.F. p. 282.

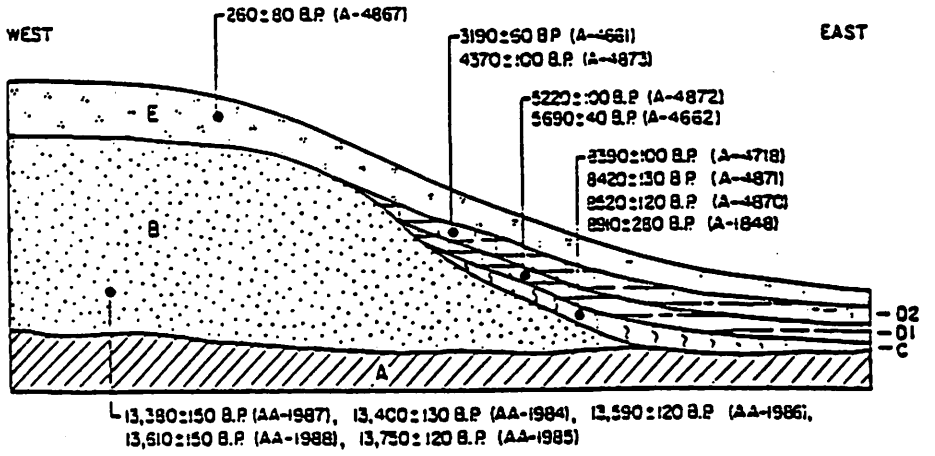


Figure 5 . Generalized geologic cross section through the western shoreline of Lake Cochise showing major stratigraphic units and some associated radiocarbon dates (not to scale).

From Waters, M & Woosley, A, p. 166.

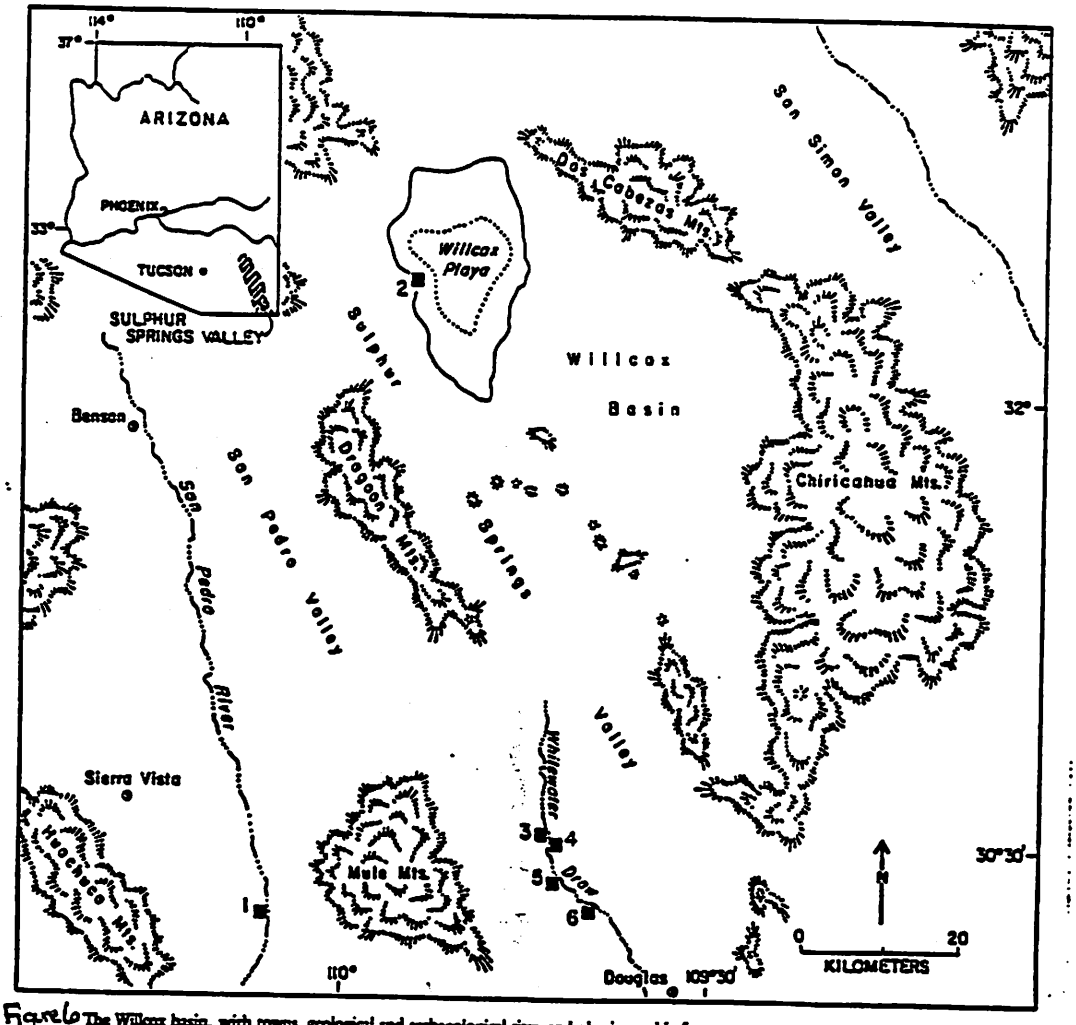


Figure 6 The Willcox basin, with towns, geological and archaeological sites, and physiographic features mentioned in the text. The Willcox Playa (dotted line) and the 1274 m shorelines of Pleistocene Lake Cochise (solid line) are indicated. 1: Lehner Clovis site; 2: Sites AZ CC:13:3, AZ CC:13:5, AZ CC:13:66, and gravel pits along Lake Cochise shoreline; 3: Sulphur Spring site AZ FF:6:9; 4: Sulphur Spring site AZ FF:6:8, 5: Sulphur Spring site AZ FF:10:1 (Double Adobe); 6: Sulphur Spring site AZ FF:10:14. Hatched area on the inset indicates position of the Sulphur Springs Valley in SE Arizona.

From Waters, M & Woosley, A, p. 164.

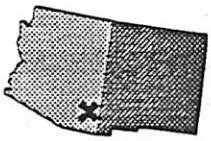

# Clay Dunes of Wilcox Playa
## Bill Bottke, Moderator

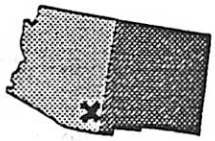

## Basic Review of Playas

Playas are flat and barren lower portions of arid basins that periodically flood and accumulate sediment. They only form in climates which sustain high annual evaporation/precipitation ratios (often 10:1). Seasonal flooding and evaporation often leave a thin layer of fine mud on the valley floor, which dries in the sun to form a very flat, dry lake bed of hard, mud-cracked clay. This surface layer may also be covered with a bright white layer of dried salt if (1) the playa's runoff contained a large amount of dissolved salt or (2) the seeping ground water brought salt to the surface.

## Clay Particles and Wind Transport


- The dry mud flats are composed primarily of small clay particles (~ 4 μm).
- For small particles, **suspension** dominates transport. Earth's atmospheric density and wind velocity are insufficient for the clay particle transport by **saltation**.
- Consequently, any wind strong enough to lift a clay particle would carry it away from the playa.

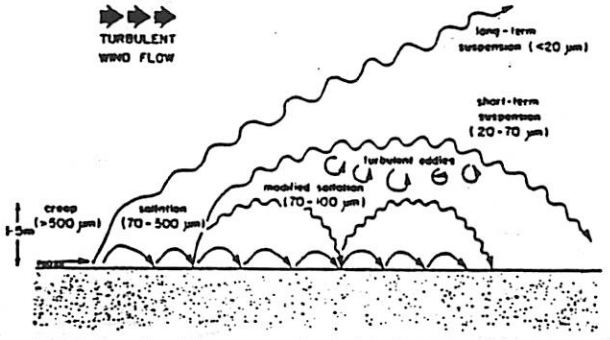


*Figure 3.9. Modes of particle transport by wind. Indicated particle-size ranges in different transport modes are those typically found during moderate windstorms ($\epsilon = 10^{-4}$–$10^{-1}$ cm$^2$ s$^{-1}$).*


- Particle movement in the atmosphere is dependant on atmospheric density, wind velocity, and particle size.
- The difficulty in picking up small particles increases with decreasing grain size.
- Big particles can be easier to move than small particles if particle size is larger than each "air" sublayer size.

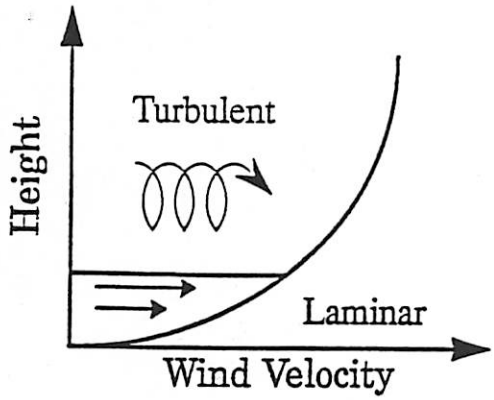


**Turbulent Flow:** Non-regular fluid motion. Eddies, rapid interchange of momentum. Particle suspension.

**Laminar Flow:** Steady flow, fluid moves in parallel layers. Difficult to pick up small particles.

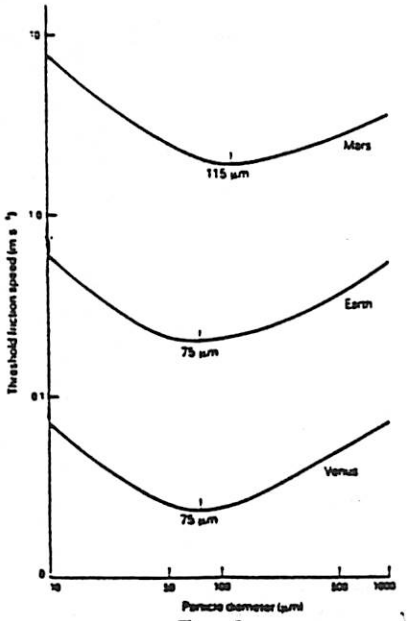


Figure 2

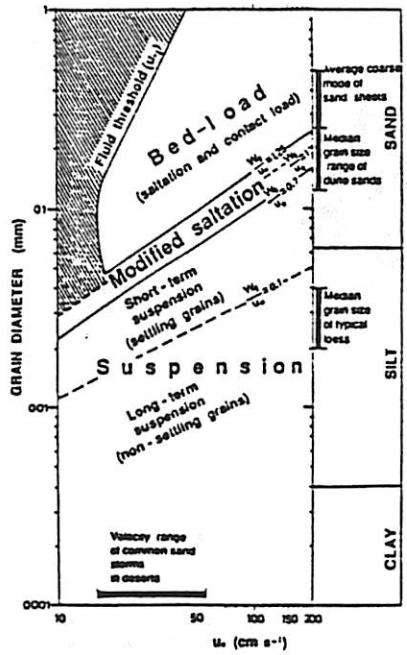


Figure 4.18 Modes of transport of quartz spheres at different wind shear velocities. (After Tanner & Pye 1987).

## Clay Aggregates

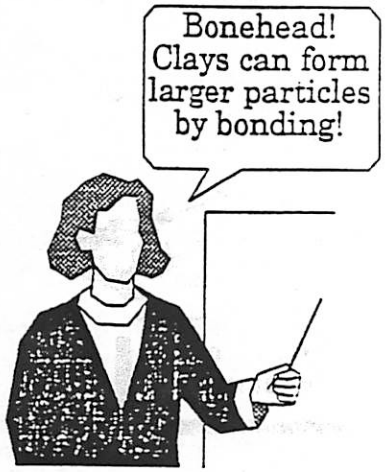


- Along the margins of drying salt flats, aggregates of clay minerals are formed by the processes of mud cracking, salt crystallization, and hydration.
- These clay pellets can be sand-sized (62-250 μm), allowing saltation to occur.
- Salt is a necessary component, since it cements clay particles, prevents vegetation and promotes blistering of the playa's mud.

## Composition of Clay Aggregates

Typical clay pellet composition consists of clay and quartz, with a mixture of minerals including kaolinite, illite, smectite and mixed-layer clay, chlorite, feldspar, and carbonates. Dunes of Wilcox Playa contain laminae of quartz sand and felspar (with) playa crust fragments, making them analogous to the Texas Gulf Coast clay dunes.

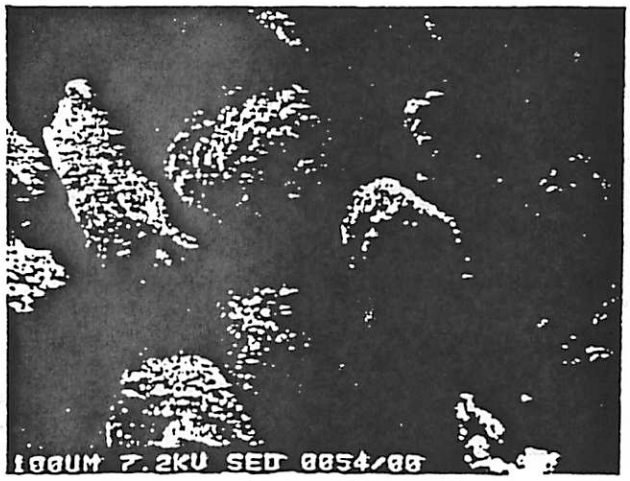


**Figure 3.28** Scanning electron micrograph showing sand-size clay pellets from the shores of a saline lake, Argentina (sample collected by A. T. Grove). Scale bars = 100 μm.

## Formation of Clay Dunes

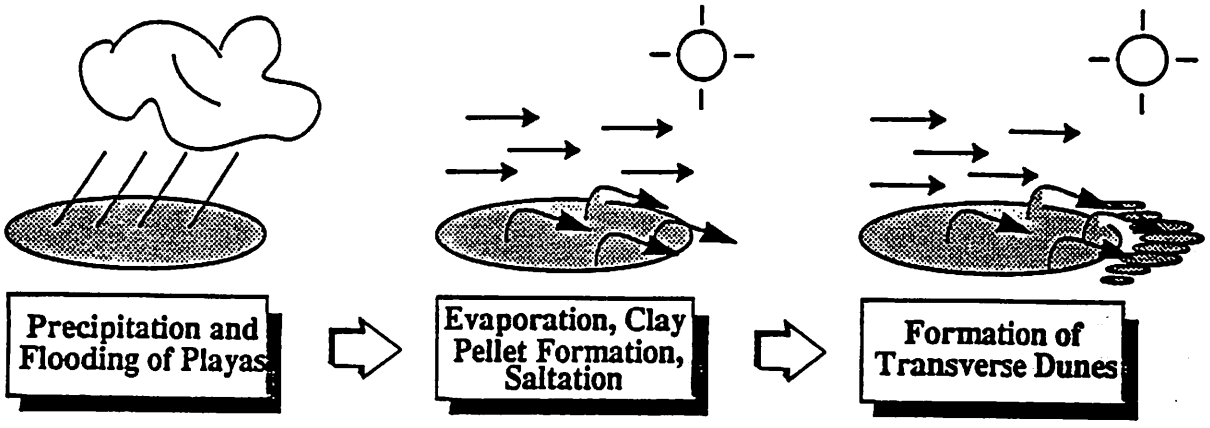


*Three main factors are involved in the formation of all clay dunes:*

1. Saline environments
   - Salts inhibits vegetation which would trap aeolian sediment on the dry playa surface.
   - Efflorescence of salts in exposed surface clays produces sand-sized clay pellets.
2. Seasonal flooding
   - Flooding promotes new clay aggregate formation.
   - It also prevents vegetation from forming on the playa.
3. Rapid drying followed by deflation
   - High evaporation rates lower the region's water table, exposing a wide expanse of bare mud flats.
   - High temperatures dry the muds and produce the efflorescence of salts needed to form clay aggregates.
   - Rapid drying is also needed, since saltation must occur before the onset of the next humid season, where the clay pellets become stabilized by hygroscopic absorption.

## Formation of Clay Dunes, cont.

Clay dune formation is restricted to regions with seasonally high evaporation rates. For example, the mean temperature of the hottest months where clay dunes form in Texas is 28.7 °C. After seasonal flooding and evaporation, clays break down to form a layer of fluffy pellets which are then transported by strong dry winds to the margin of the salt flats. It is important to note that dune formation is also aided by a season of strong and unidirectional winds. Accumulation of the clay pellets occurs where the surface has been stabilized to some degree (*i.e.* vegetation, fences, rough terrain, *etc.*). The subsequent formation is a transverse dune ridge. However, the clay dunes formed have morphological and structural features significantly different than quartz dunes (QD).

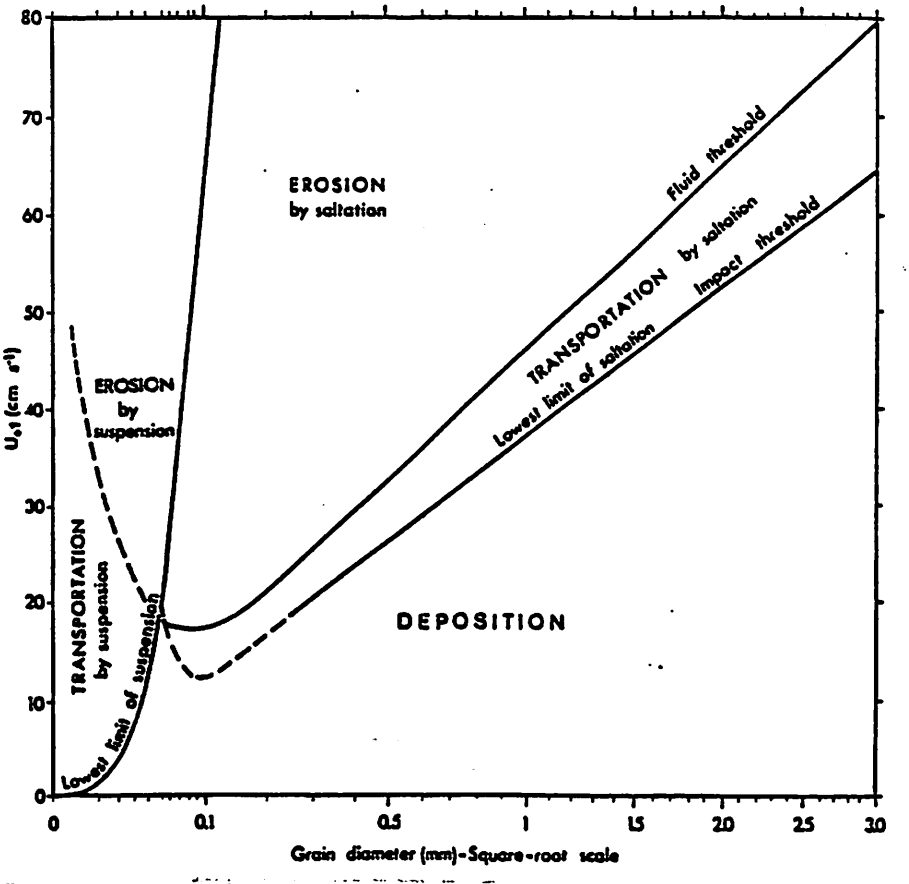


Figure 4.4 Variation of the fluid threshold velocity and the impact threshold velocity with grain size. The distinctions between the saltation and suspension modes of transport, and between erosion, transportation, and deposition, are also shown. (Data partly from Bagnold 1941, p. 88, and Chepil 1945b).

## Characteristics of Clay Dunes

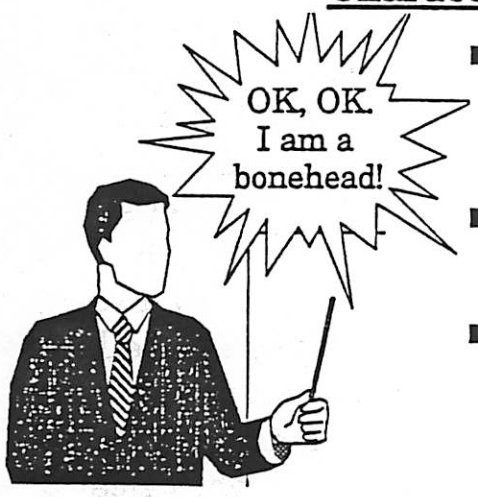


- Clay dunes are transverse to dominant wind direction and they do not migrate from the source area (unlike QD).
- Typical sizes rarely exceed 20 m in height (5-15 m common).
- Leeward slopes are very gentle, while the windward slopes are steep (opposite QD).

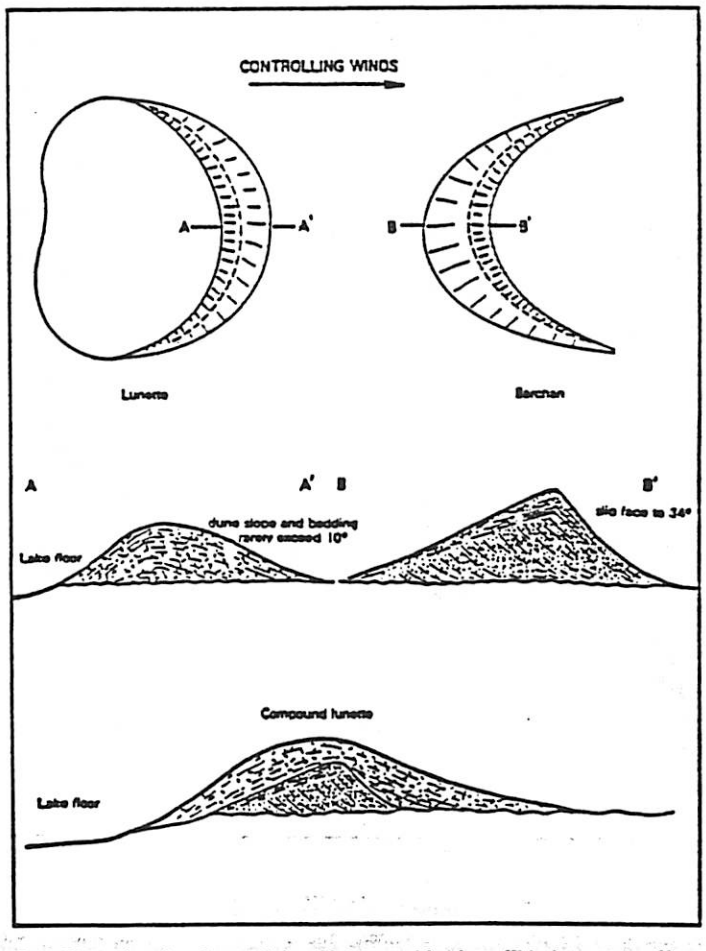


Fig. 2. Plan and section characteristics of lunettes and barchans. High clay content of lunettes largely determines their plan orientation, cross-section morphology and bedding characteristics. Compound lunettes representing two separate hydrologic environments, a high-water, quartz sand facies and a low-water, saline facies (clay-rich component), are present on some lakes in southeastern Australia.

## Dune Structure

The slope of the dunes is a consequence of clay aggregates affecting the depositional processes:

- *Layered accretion:* The seasonal absorption of moisture by the clay aggregates prevents further movement of last season's accretion layer. Thus, the thick accumulations of mobile aggregates necessary for generating large slip faces (as in QD) do not normally develop.
- The thin layer accumulated next season already has a stabilized surface. This layer-by-layer accretion generates dune topography and controls the internal structure.
- The seasonality of stability and the consequent inability to form deep mobile deposits prevent clay dunes from migrating from their immediate source. This is different from QD which form parabolic dunes on the downwind margin of lake shore.
- Thus the presence of low-angle planar beds and absence of cross-sets in clay dunes in consistent with the absence of steep downward slopes from their surface morphology.

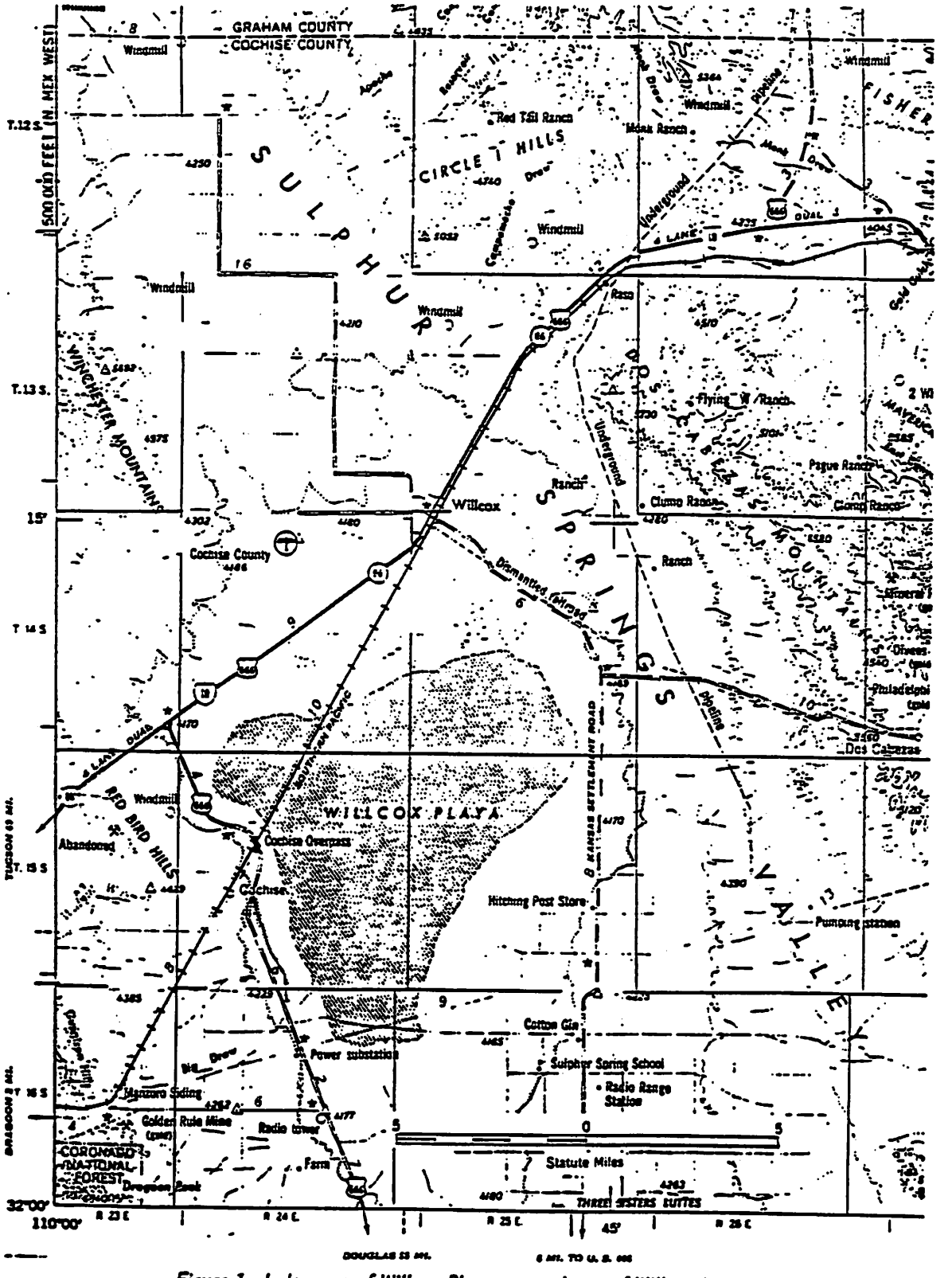


*Figure 1. Index map of Willcox Playa area and part of Willcox basin.*

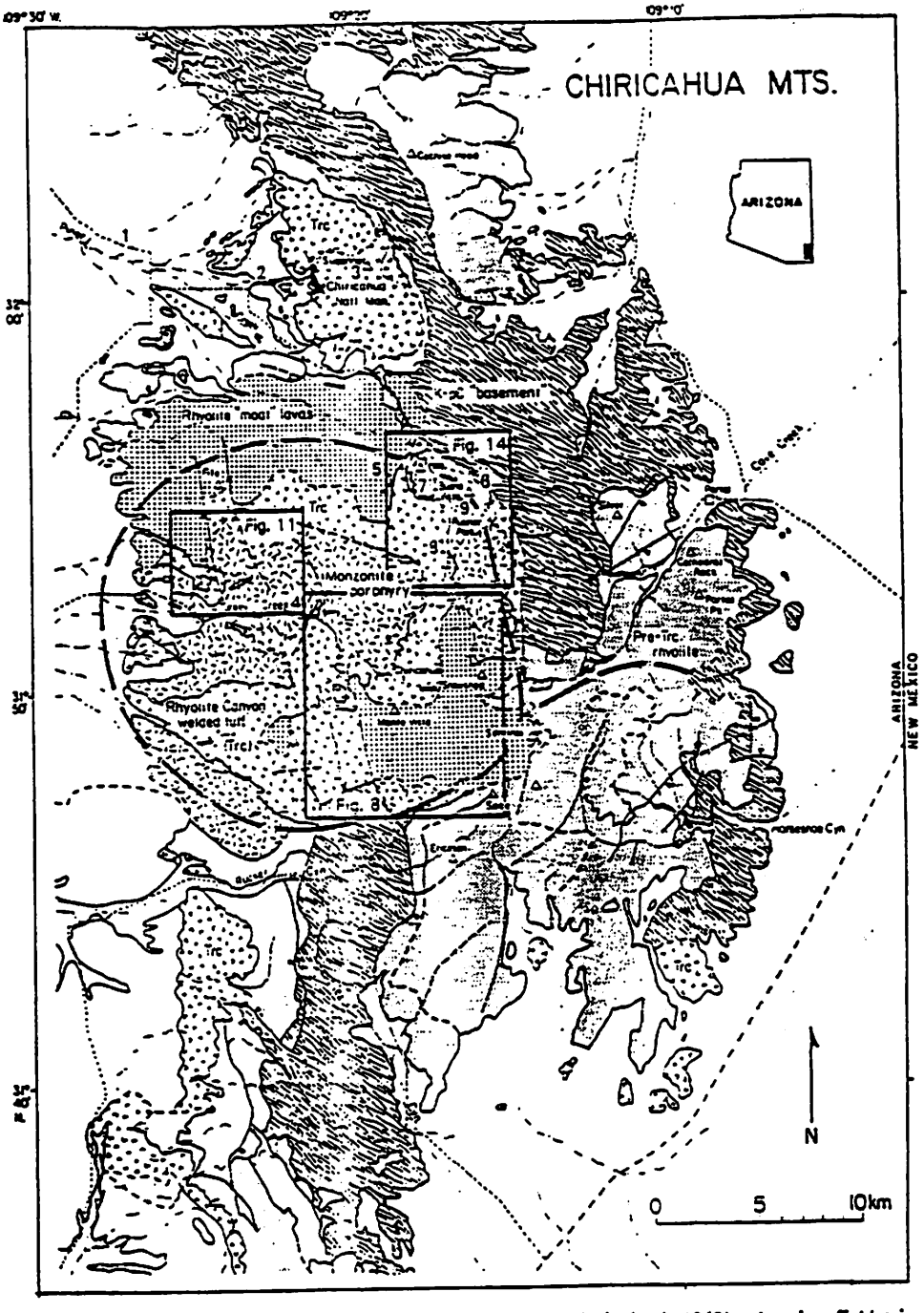


Figure 1. Geologic index map of the Chiricahua Mountains (after Marjaniemi, 1969), showing field trip localities (by number) and areas of more detailed map figures. Trc = welded tuff of Rhyolite Canyon Formation; K-pC = Cretaceous to Precambrian rocks. Approximate structural boundary of the Turkey Creek caldera, and NW boundary of the Portal caldera indicated by heavy lines.

units. These preliminary results suggest that unit I may have been separated by at least a few hundred years from units II and III, and that unit I may contain more than one cooling unit. Nevertheless, the overall tight clustering of the data is consistent with origin of all the rocks in a relatively short period of time; all of the directional variation can be explained by secular variation.

Latta recognized a depositional break within the intracaldera tuff, and, on the basis of major-element chemistry, he correlated the *lower* depositional unit of the intracaldera sequence with his *upper* unit of the outflow tuff (Monument member, unit III) (Figure 5), leaving correlation of the upper unit of the intracaldera tuff and the two lower depositional units of the outflow tuff in question. He suggested that the later part of the main eruptive sequence (upper unit of intracaldera tuff) ponded in the caldera and that the outflow sequence includes units erupted before and after caldera collapse. The lower ash flow units of the outflow tuff may have erupted during the initial stages of caldera formation, prior to significant collapse, and accordingly are not preserved inside the caldera; alternatively, they may exist in the subsurface, below a monzonite porphyry sill (see discussion). We also note the chemical similarity of the upper cooling unit of the outflow sequence with the intracaldera tuff. Although there is considerable variation in the alkalis and rubidium, the more immobile elements show good agreement between the two units (Table 1).

Dacite lava overlying the ash-flow sequence in the National Monument (dacite of Sugarloaf Mountain) is chemically and petrographically similar to porphyry of the ring intrusion and to the earliest lavas erupted from the ring intrusion of the caldera at Barfoot Peak (Table 1; locality is near Ida Peak on Figure 1). Because of the lack of vent structures closer to Sugarloaf Moun-

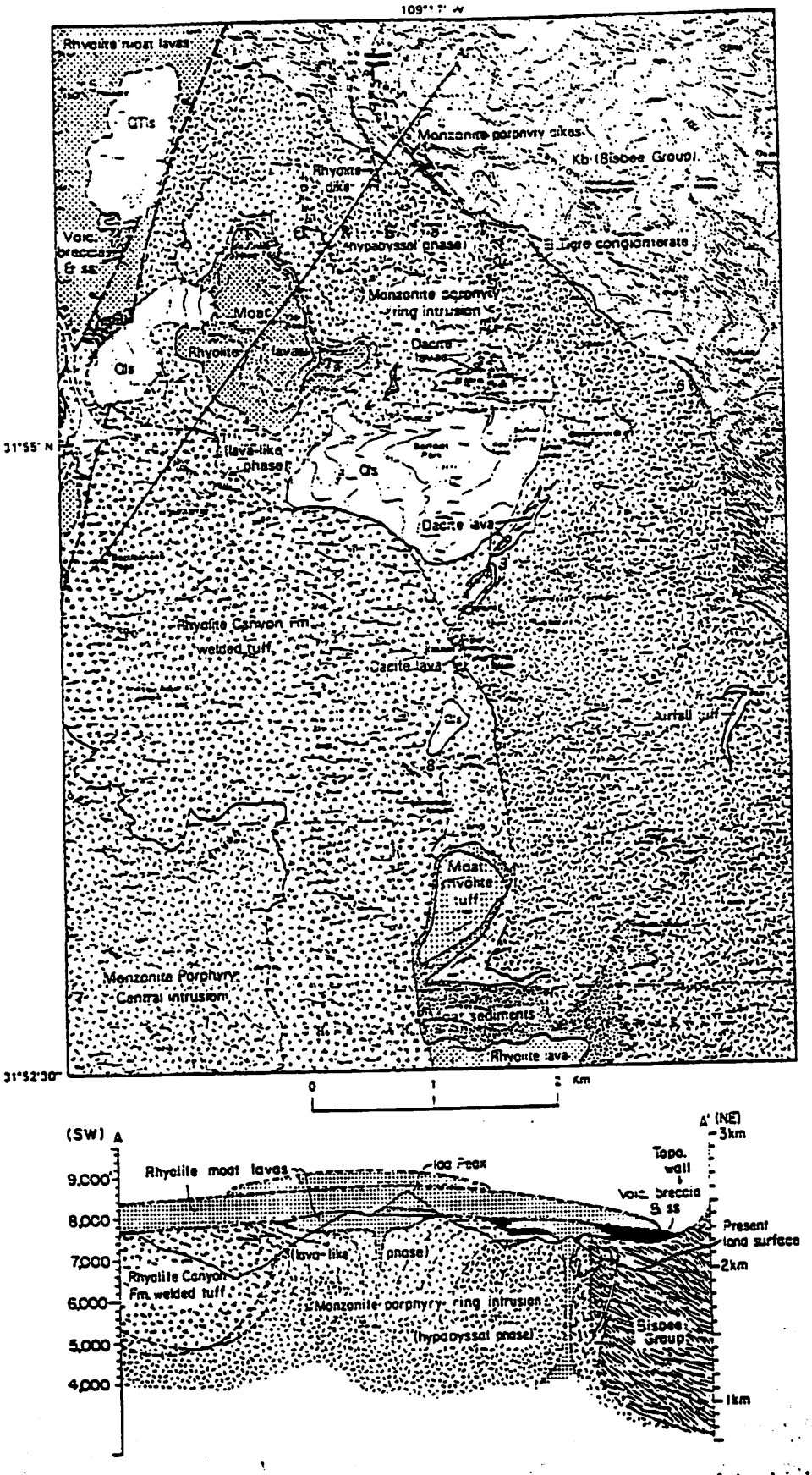


**Figure 9. Geologic map (a) and interpretative cross section (b) of the northeastern segment of the ring intrusion, Turkey Creek caldera. Field trip localities are indicated by stop number. Profile line shows present topography. Stippled areas represent carapace breccia. Qls = Quaternary landslide deposit, QTls = Quaternary or Tertiary landslide deposit. El Tigre conglomerate, an informal unite of Tsugii (1984).**

the moat sequence that caps Ida Peak. east (toward Barfoot Peak). This traverse through flow-foided rhyolite lava and lower the lower moat-rhyolite, then into platy- nzonite porphyry with local remnants of moat erosional(?) surface, and finally into glass-matrix that cap Barfoot Peak. *Please keep together*; we will to the top of Barfoot Peak, instead congregate on the spur ridge, then "peel off" to the south to intercept the k trail back to the cars.

Stop 8 -- Ring dike feeder zone

Backtrack 0.8 mi on the Barfoot Park Road, *leave one vehicle at the Barfoot lookout (Buena Vista Peak) trailhead* (at the cattle-guard), then proceed 0.2 mi to the Rustler Park Road, turn right (south) and drive 1.0 mi to the Barfoot Campground; continue south, past the cabins and on the 4-wheel-drive road 1.0 mi, turn right (uphill) on side road, proceed 0.1 mi, veer right and continue another 0.1 mi to Bootlegger Saddle. Hike north, up the west face of the ridge, through vesicular and lavalike platy weathering monzonite (dacite) porphyry for about 0.2 mi to the prominent spur west of Hillside Spring (Figure 9). Descend 100 ft in elevation (to the west) on the spur to a prominent low cliff and hoodoo that mark the contact between monzonite porphyry of the ring intrusion and intracaldera tuff.

Look carefully at the monzonite porphyry as you descend to the cliff; this rock has a subhorizontal platy jointing and eutaxitic-like structure. Interlayered zones of pumiceous(?) quartz-free monzonite/dacite porphyry with and without feldspar megacrysts are present. The cliff is composed primarily of spherulitic quartz-sanidine rhyolite that locally preserves ghost-like flow banding, flow folds(?) and spatter breccia fragments. A few meters below the top of the cliff (to the south) is an outcrop containing a 30-cm-diameter block of quartz-bearing feldspar megacrystic pumice. The pumice is chemically similar the tuff of Rhyolite Canyon, although it has anomalously high MgO, CaO, MnO, and Sr and high La, Ce, and Nd (Table 1). *Please do not collect here, as this is a rare occurrence.*

These outcrops are interpreted as pyroclastic spatter breccia that locally forms the inboard margin of the monzonite porphyry ring intrusion. Both the inboard and outboard contacts of the intrusion form steep slopes that are generally obscured by talus, however, in both situations isolated outcrops of breccia have been found. Similar outcrops of pyroclastic and reworked breccia were observed near the outboard side of the ring intrusion, north of Barfoot Peak, and near Flys Park (0.8 mi SSE of here, Figure 9). These outcrops suggest that the true width of the ring dike at depth may locally be less than a few hundred meters, and that the several-km-wide band of porphyry exposed at the surface is accentuated in width by dome and lava flow infilling of the caldera moat. This relation is also suggested by the flow-like partings and intercalated airfall tuff within the monzonite porphyry exposed in the cliffs below Centella Point, Barfoot Peak and Ida Peak.

Samples of dark and light zones within banded breccia blocks in outcrops near Flys Park have chemical compositions that suggest mingling of high-silica Rhyolite Canyon tuff magma with monzonite porphyry magma (Table 1). Dark grey dacitic flame or magma blebs that are similar to monzonite porphyry (by virtue of containing feldspar megacrysts and fine-grained lithic inclusions) are also common in the upper part of the intracaldera tuff. These relations suggest a transition in eruptive style within ring vents that initially erupted the tuff of Rhyolite canyon, then dacite (monzonite) porphyry.

Stop 9 -- "String of Pearls"

Return to the cars and backtrack to the Rustler Park Campground. Hike northwest from the campground and intercept the ridge trail to Buena Vista Peak. *Please keep together.* We will follow the crest of the ridge (above and parallel to the trail) from the first saddle to the trail forks at the saddle just south of Buena Vista Peak (Figure 9). We then take the right fork and descend to the car we left at the Barfoot Lookout (Buena Vista Peak) trailhead. Drivers will be ferried back for the vehicles. *If you get lost or separated* descend to the *east*. You should cross the Rustler Park-Buena Vista Peak trail just below the ridge crest, then the Rustler Park Road, 200 to 350' (elevation) below the crest.

This traverse takes us through the "String of Pearls", a series of dacite porphyry lava domes atop the monzonite porphyry ring dike. These are interpreted as the extrusive equivalents of the monzonite porphyry. They have glassy basal/marginal carapace breccias, and show similar relations to those seen at Barfoot Peak (Stop 7). Excellent overviews of the caldera to the west and north are available from the ridge crest.

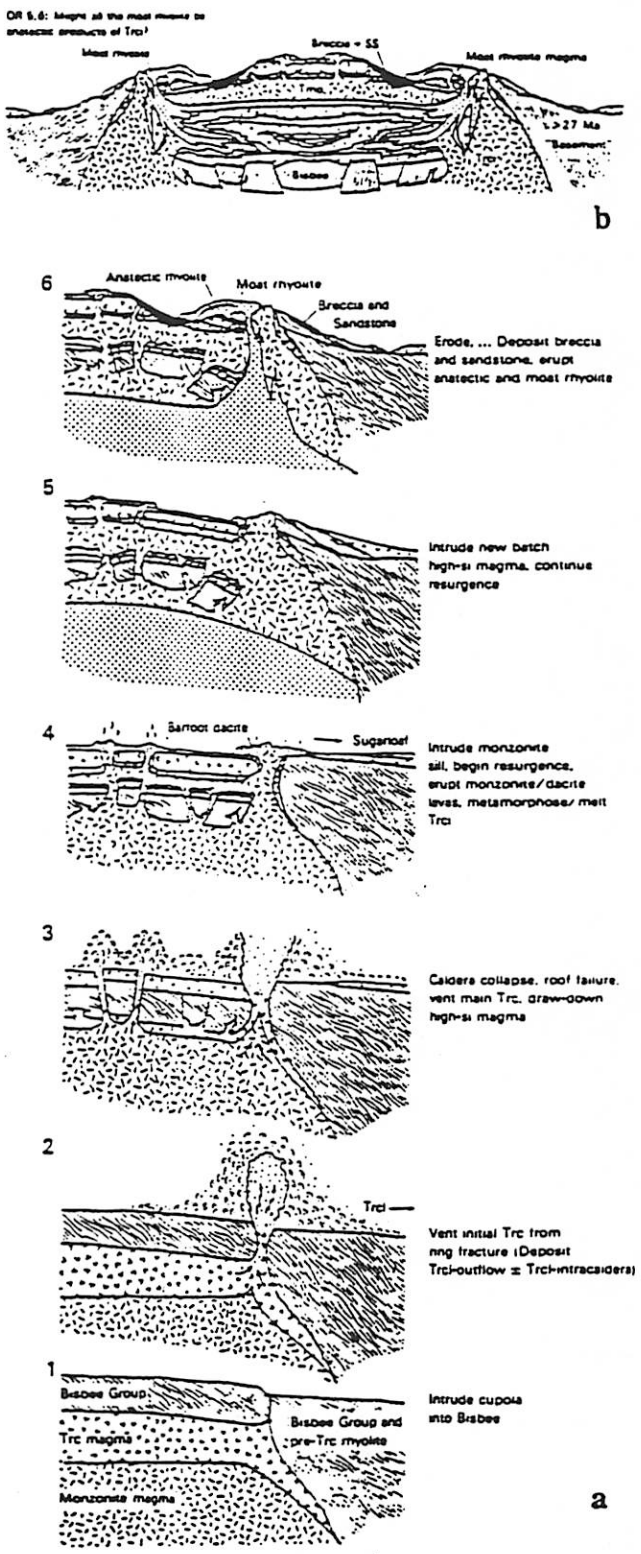


Figure 10. Working models for structural stages in the evolution of the Turkey Creek caldera. (a) batch model; (b) anatectic model for stages 5 and 6. Trc = tuff of Rhyolite Canyon Formation; Trcl = lower members (units I and II of Latta (1983) of outflow tuff of Rhyolite Canyon Formation); Trci = intracaldera facies tuff of Rhyolite Canyon Formation; Tmp = monzonite porphyry.

# Day 2:

# Chiricahuas to Socorro

Yer /
Road Log:
Lordsburg - Las Cruces

with your
excellent host,
Andy Rivkin

Partn. Jay /

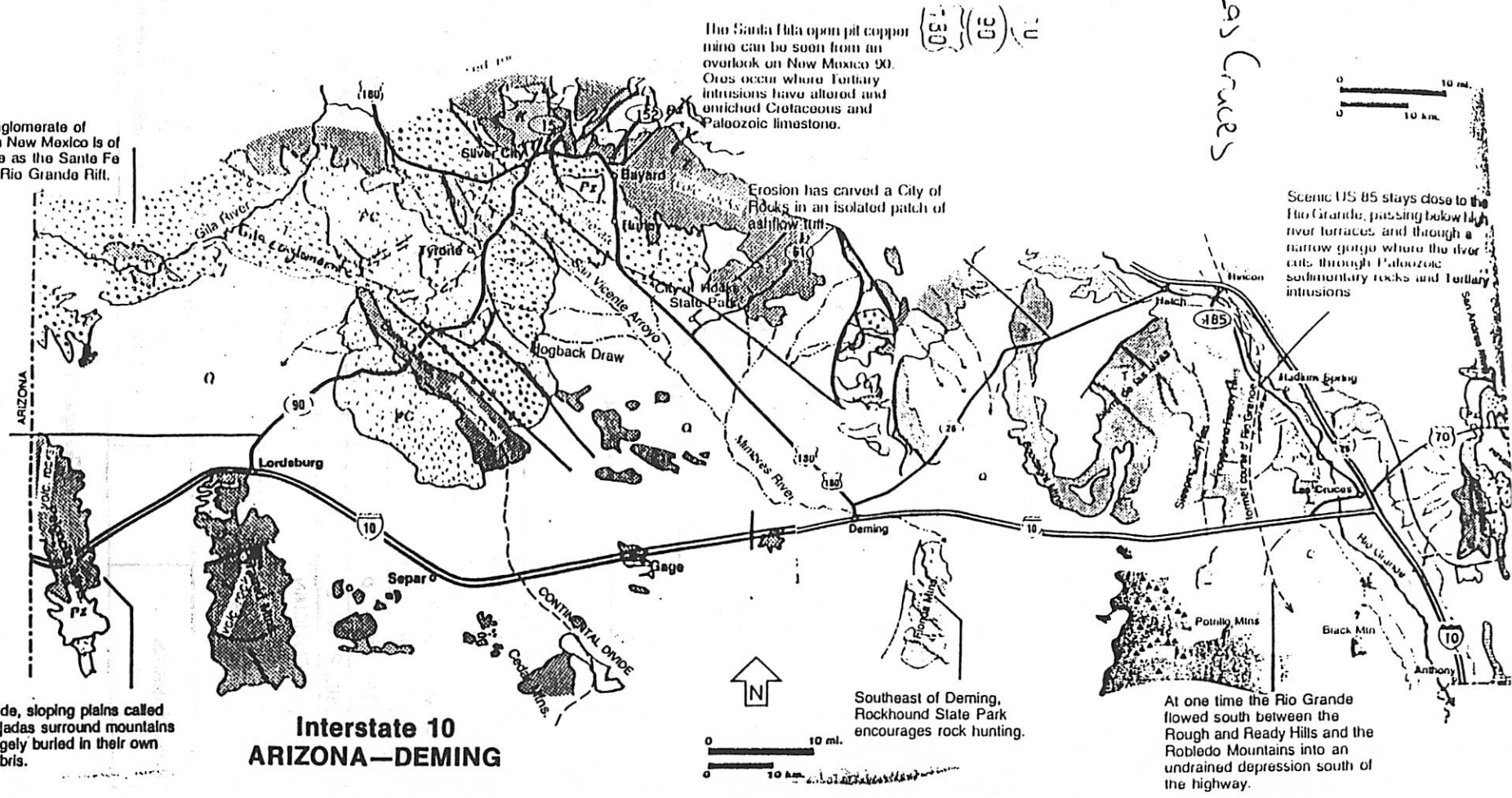


**Interstate 10**
**ARIZONA—DEMING**

| ERA | PERIOD | EPOCH | AGE | EVENTS IN NEW MEXICO |
|---|---|---|---|---|
| CENOZOIC Age of Mammals | QUATERNARY Q | Recent | | Present erosion cycle trenches Pleistocene deposits, partly refills Rio Grande Rift valley. Basalt eruptions build cinder cones and lava flows near Grants, Carrizozo, and Capulin. |
| | | Pleistocene | .01 | Cyclic erosion, product of repeated glacial cycles farther north, alternately trenches and fills the Rio Grande Valley. Small mountain glaciers develop in northern New Mexico mountains. Jemez volcano erupts and collapses. |
| | TERTIARY T | Pliocene | 2 | Basins between ranges fill with debris eroded from surrounding mountains. Some drainage integrates: the Rio Grande becomes a through-flowing stream. |
| | | Miocene | 5 | Increasing crustal tension creates basins and ranges of southern New Mexico. Intense volcanism builds and destroys many large volcanoes in the southwest part of the state. |
| | | Oligocene | 24 | The Rio Grande Rift begins to sink between two sets of faults. West of the still-sinking San Juan Basin, plateaus develop. |
| | | Eocene | 37 | Debris from the Rocky Mountains fills the San Juan Basin. Mammals diversify, diversify, many the ancestors of modern forms. |
| | | Paleocene | 58 | Continued rise of Rocky Mountains and initial sinking of San Juan Basin accompanies westward drift of continent. Mammals flourish on land. Mineral-bearing intrusions form in parts of the state. |
| MESOZOIC Age of Reptiles | CRETACEOUS K | | 66 | North America breaks away from Europe and starts to drift westward. Briefly, a vast sea covers parts of New Mexico. The Rocky Mountains rise to the north. Finally, a great extinction annihilates many forms of life, ending the Age of Reptiles. |
| | JURASSIC J | | 144 | Seas of sand sweep in wide deserts across northern New Mexico. Dinosaurs roam river floodplains and near-shore marshes. |
| | TRIASSIC $\overline{TR}$ | | 208 | Coastal plain, floodplain, and delta deposits spread across state, their sediments derived from ancestral Rockies. Explosive volcanism adds volcanic ash to these sediments. Dinosaurs appear. |
| PALEOZOIC Age of Fishes | PERMIAN P | | 245 | Southern seas advance across much of New Mexico. A large barrier reef develops in the south, followed by drying up of the sea and creation of extensive salt and gypsum deposits. Locally, erosion removes some earlier sedimentary layers. |
| | PENNSYLVANIAN $\overline{IP}$ | | 286 | A southern sea covers much of New Mexico with sand, mud, and limestone. With the rise of the ancestral Rockies, sediments become coarser. |
| | MISSISSIPPIAN M | | 330 | Widespread deposition of fossil-bearing marine limestone is followed by uplift and development of karst topography with solution caverns and sinks. |
| | DEVONIAN D | | 360 | Marine deposits—limestone and shale—form in shallow seas. |
| | SILURIAN S | | 408 | Marine deposits form. Most are later eroded away. |
| | ORDOVICIAN O | | 438 | Marine deposits—limestone and shale—form in shallow seas. The first fishes appear. |
| | CAMBRIAN C | | 505 | A western sea advances across the stripped Precambrian surface, depositing sandstone, shale and limestone. Shellfish are widespread and abundant: the Age of Fishes has begun. |
| PRECAMBRIAN pC | | | 570 | Episodes of mountain-building and volcanism alternate with periods of marine and non-marine sedimentation. Intrusions of granite occurred roughly 1.35 billion years ago. Finally, a long period of erosion flattens the landscape. |

*Geologic calendar*

Geologic Map - Florida Mts.

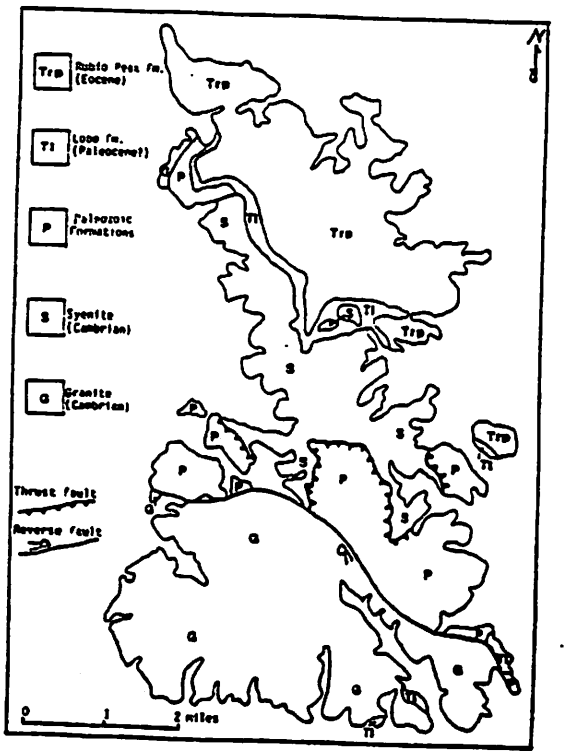


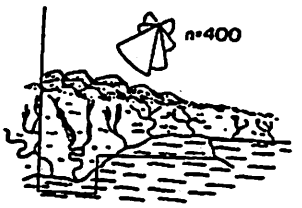


A. Middle Hell-to-Finish Time

B. Early U-Bar Time

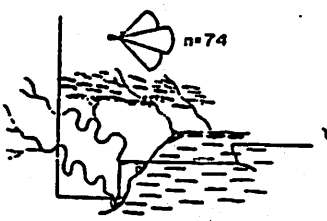


C. Middle Mojado Time

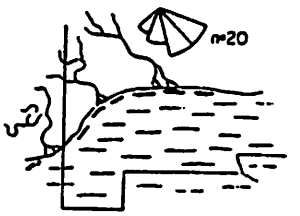


D. Late Mojado Time

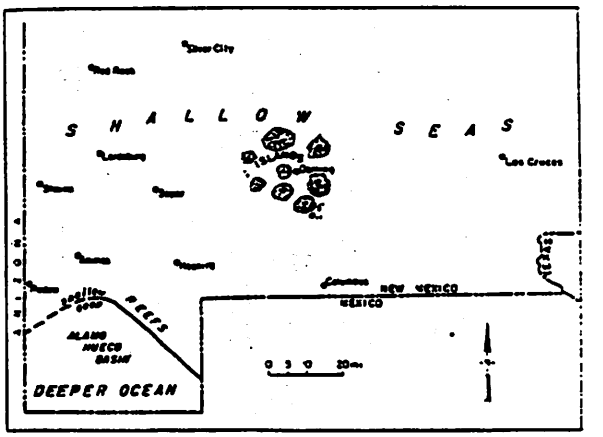


PALEOGEOGRAPHIC MAP OF SOUTHWESTERN NEW MEXICO DURING PART OF PENNSYLVANIAN TIME.

Figure 4. Early Cretaceous paleogeographic maps, southwestern New Mexico. A) Middle Hell-to-Finish time. Mountains represent the Burro uplift. Paleocurrent rose represents 400 imbrication measurements from cobble conglomerates in the Little Hatchet Mountains. B) Early U-Bar time. C) Middle Mojado time. Paleocurrent rose represents 62 trough cross-bed and 12 parting lineation measurements from point-bar sandstones in the Big Hatchet and Animas Mountains. D) Late Mojado time. Paleocurrent rose represents 20 trough and planar crossbed measurements from the Sarten Formation in Cooke's Range.

p. 3

Stansberry Cenozoic Extension in the Southwest

## Tectonic Setting

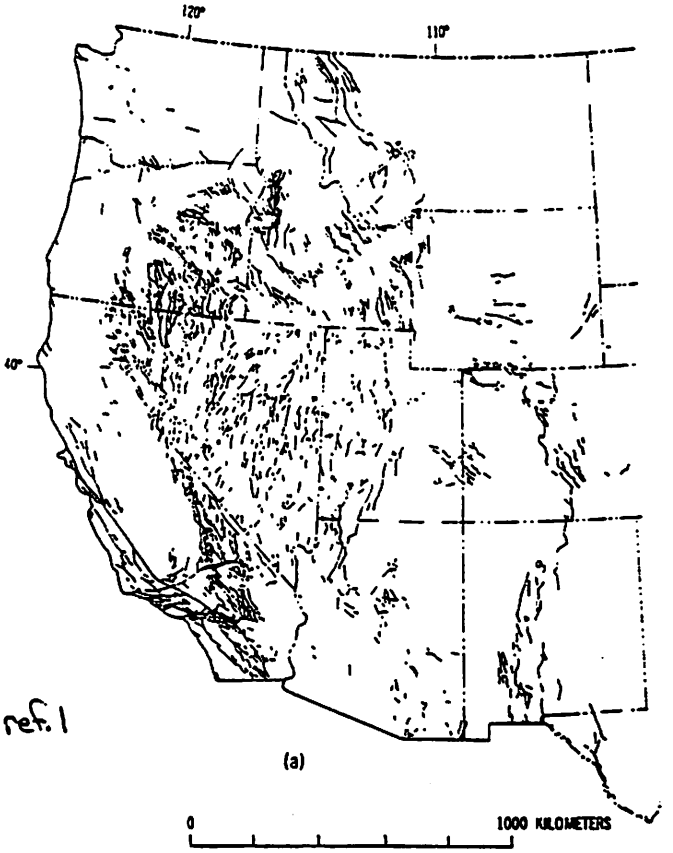


ref. 1

Figure 2 - Fault systems of western North America:
a, faults known or believed to have been active in the past 10 to 15 m.y. for which possible Quaternary movement is suspected (after Howard and others, 1978);

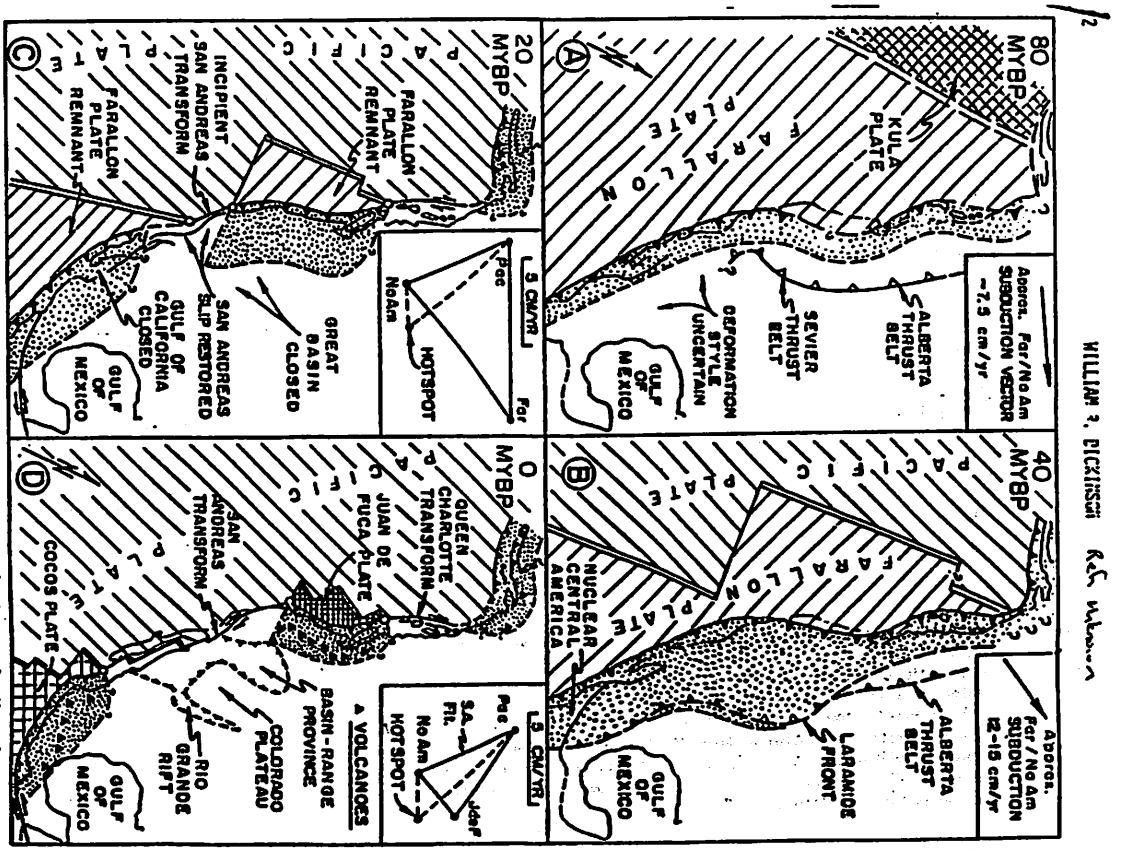


Figure 1. Inferred plate configurations and plate motions (insets). See text for discussion.

WILLIAM R. DICKINSON Ref. Volcanism

(1)

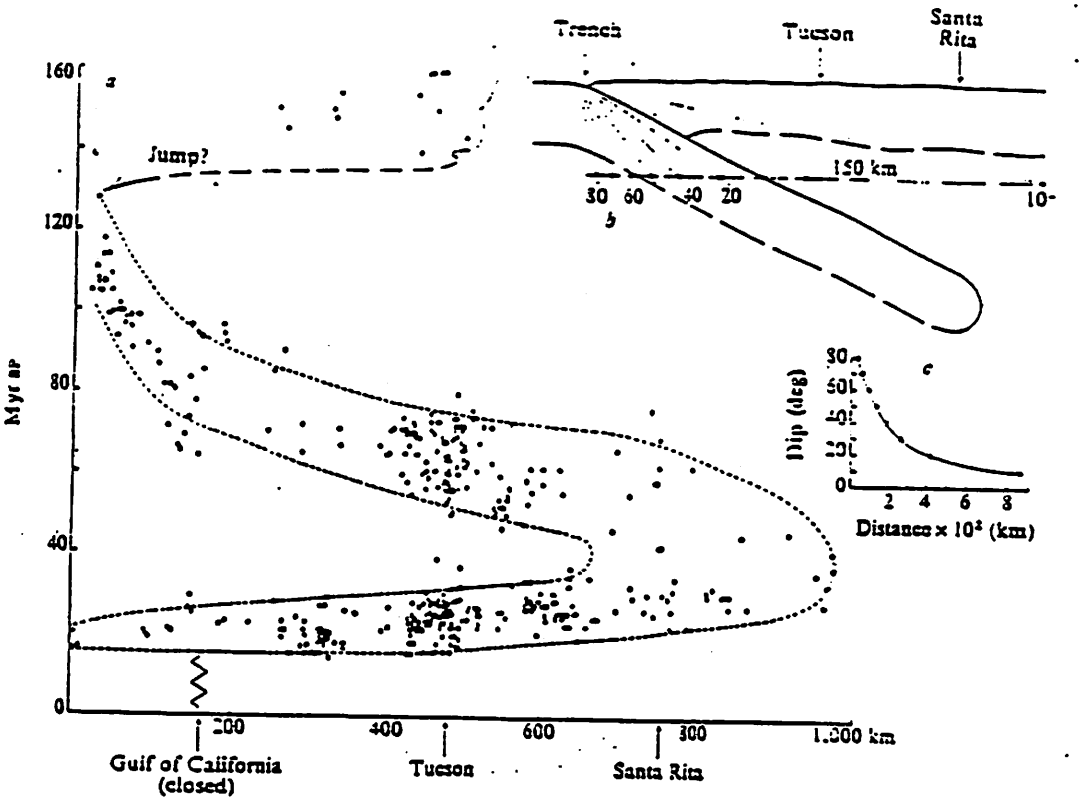


Fig. 2 *a*, Distribution of radiometric ages from Fig. 1 plotted as a function of time. Dates projected into a line passing through Tucson, Arizona, and Santa Rita, New Mexico after closure of Gulf of California. ○, single mineral K/Ar ages on plutons in southeastern California. *b*, Hypothetical arc-trench system scaled to southwestern North America. Various dip-angles of Benioff zones shown with points of intersection with 150 km depth line. *c*, Graphical representation of function controlling distance from trench to magmatic arc with varying Benioff zone dip angles.

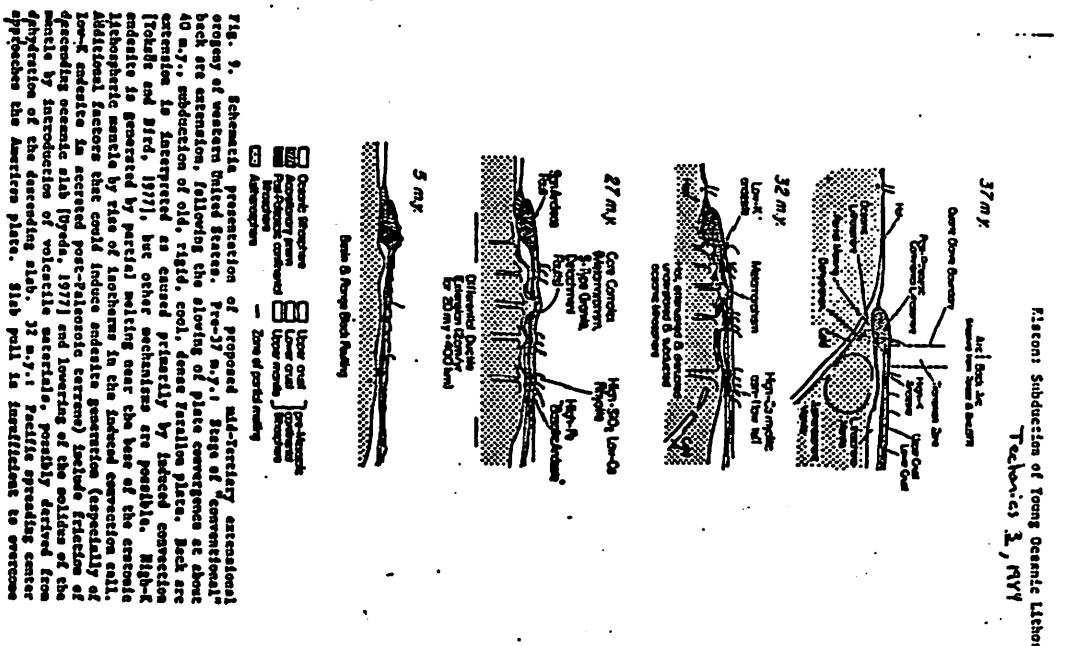


Fig. 9. Schematic presentation of proposed mid-Tertiary extensional orogeny of western United States. Pre-37 m.y. stage of "conventional" back arc extension, following the slowing of plate convergence at about 40 m.y., subduction of old, rigid, cool, dense Farallon plate. Back arc extension is interpreted as caused primarily by induced convection (Toksöz and Bird, 1977), but other mechanisms are possible. High-K andesite is generated by partial melting near the base of the central lithospheric mantle by rise of isotherms in the induced convection cell. Additional factors that could induce andesite generation (especially of low-K andesite in accreted post-Paleozoic terrane) include friction of descending oceanic slab (Oyarzo, 1977) and lowering of the solidus of the mantle by introduction of volatile materials, possibly derived from dehydration of the descending slab. 32 m.y.: Pacific spreading center approaches the American plate. Slab pull is insufficient to overcome

Plateau Subduction of Young Oceanic Lithosphere
Tectonics 3, 1984

Chronologic Summary of Crustal Extension. The distribution of Cenozoic crustal spreading in time and space in the western North American plate can be summarized as follows:

(a) 30 to 20 m.y. ago.—Rapid spreading, closely spaced normal faults and fault block rotation, accompanied by eruption of basaltic andesites and high-silica rhyolites, took place in the Rio Grande rift area at shallow crustal levels (Chamberlin, 1978). Local block faulting of the shallow crust (Crowe, 1978) and regional ductile extension of the middle crust (Eaton, 1979) occurred in the Sonoran Desert section of the southern Basin and Range province. This deformation occurred within a broad calc-alkalic, volcanic arc.

ref. 1

(b) 20 to 10 m.y. ago.—Crustal rifting and normal faulting occurred throughout most of what is now the Basin and Range and Columbia Plateaus provinces, locally accompanied by the voluminous eruption of basalt. Horst and graben structure developed in the Rio Grande rift area with little tendency for fault block rotation and at a relatively slow spreading rate (Chamberlin, 1978). A lull in magmatism that occurred throughout most of the west in the first part of this period is probably indicative of a generally slowed spreading rate. Extensional deformation took place behind both the volcanic arc, which was now narrower, and the northward-growing transform boundary at the western margin of the continent.

(c) 10 m.y. ago to the present.—In the Basin and Range province, there was a restriction of extensional spreading to the Great Basin section alone. Extensional deformation continued in the Rio Grande rift, with a pronounced pulse of uplift and block faulting in the middle of this period. It was accompanied by northwest extension in the Humboldt zone of the northern Great Basin. The direction of spreading changed markedly from southwest, in the previous period, to due west and northwest, in this period. The south end of the volcanic arc migrated rapidly northward, in consonance with migration of the Mendocino triple junction. Crustal spreading continued behind both the arc and the transform boundary.

## Mechanisms

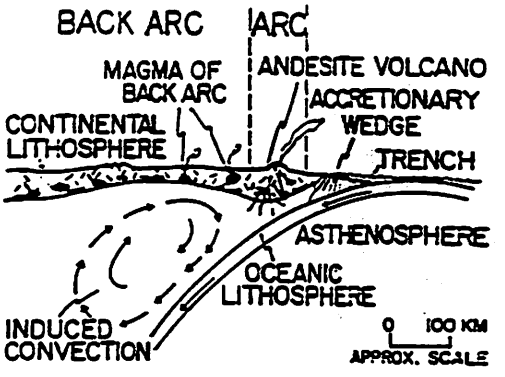


Fig. 10. Back-arc spreading of continental lithosphere by induced convection, modified from Toksöz and Bird (1977).

GRL 9, 1982

a) PHYSICAL MODEL

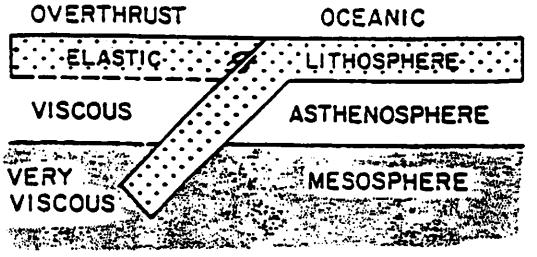


b) MATHEMATICAL IDEALIZATION

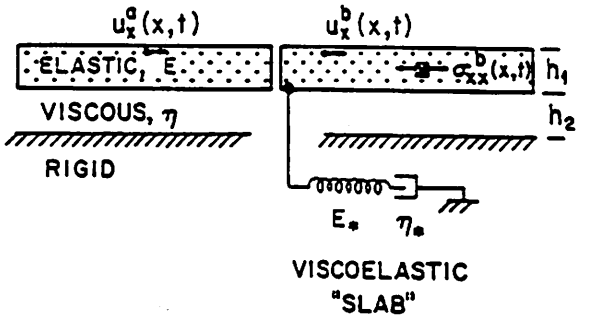


Fig. 1. Schematic diagram of (a) the principal mechanical elements in a subduction zone (assumed to be infinitely long in this paper) and (b) a mathematical idealization of these mechanical elements which incorporates both strain propagation and the effect of the subducted slab.

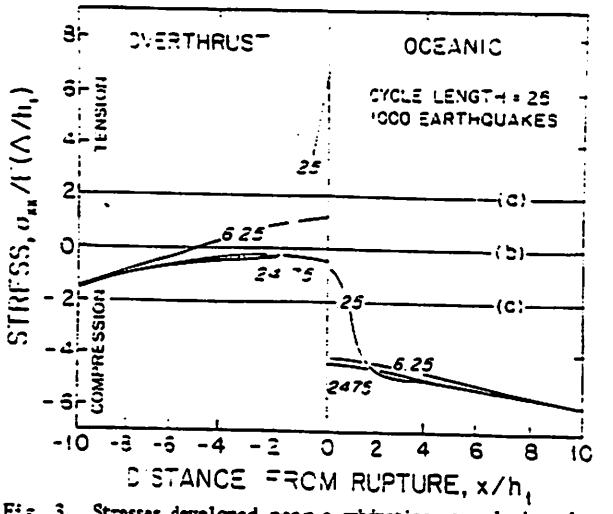


Fig. 3. Stresses developed near a subduction zone during the earthquake cycle. This is the steady state stress distribution after a series of 1,000 earthquakes which occur every 25 $\tau_a$. Curves are labeled with the number of asthenosphere Maxwell times following the earthquake, from 25 $\tau_a$ to 24.75 $\tau_a$, just before the next earthquake. Immediately following the earthquake at t = 0, note the strong extension which rapidly spreads out into the adjacent plates. The mechanical asymmetry of the subduction zone leads to a long term stress asymmetry: the stress in the overthrust plate is always more extensional than in the subducting (oceanic) plate. An arbitrary regional stress can always be added without affecting the solution: such a stress is indicated by the three alternative zero stress 'baselines' a, b, and c. The other parameters of the subduction zone are the same as for Fig. 2.

JGR 84, 1979

UYEDA AND KANAMORI BACK-ARC OPENING AND SUBDUCTION

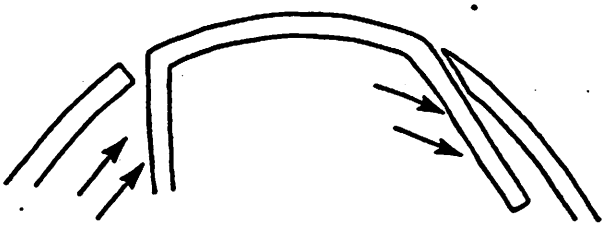

Fig. 11. An interpretation for the east-west asymmetry.

Plates globally have relative velocity w.r.t. mantle.

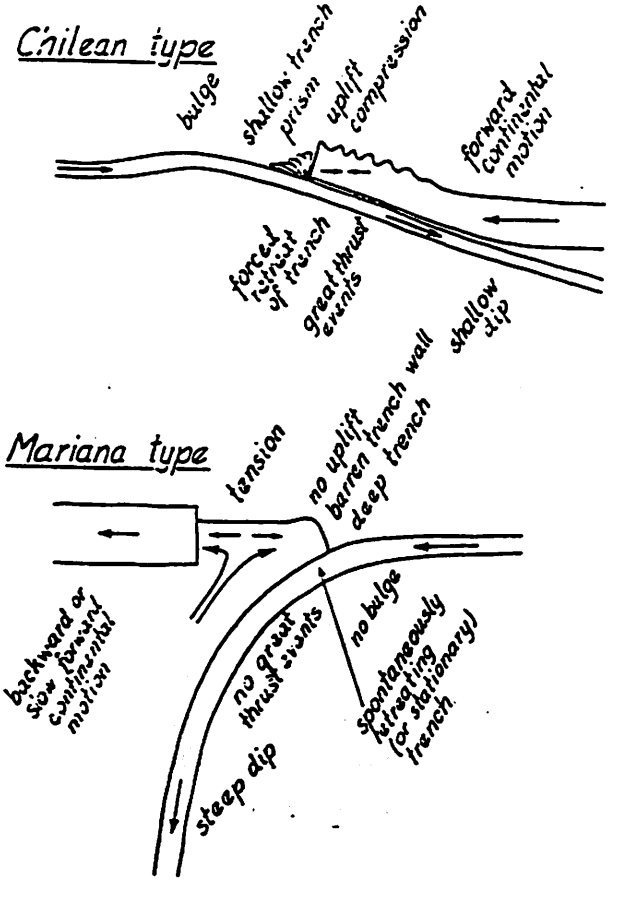


Fig. 7. Two kinds of subduction boundaries.

**Geologic History of Rio Grande Rift** Jeff Johnson

"Rift" = Elongate depressions overlying places where the entire lithosphere has ruptured in extension, resulting in regions with large crustal blocks offset by high angle normal faults.

## DESCRIPTION:

■ Extends more than 1000 km from Leadville, CO into Chihuahua, Mexico.

*North of Socorro* → rift is distinctive morpho-tectonic feature: greatest offsets ≈ 6 km along graben--north of Albuquerque (Bernalillo).

*South of Socorro* → rift is only distinguished from adjacent Basin and Range terrain by geology/geophysics (heat flow, crustal thickness from seismic data).

☐ Southern Rio Grande Rift is characterized by:

* high heat flow (> 100 $mW/m^2$)
* young (< 0.4 Ma) faults
* young (< 4-5 Ma) basaltic volcanoes
* 1.5 km+ deep basins, compared to the < 1 km deep Basin and Range (B&R) grabens.
* crustal thinning (inferred from seismic profiling and gravity anomaly studies).

■ A broad gravity low (up to -200 mgals) exists across the state upon which is superimposed a regional relatively positive Bouger gravity anomaly. In combination with the observed low crustal densities and seismic velocities, this positive gravity anomaly might be explained by a combination of crustal thinning and associated upwarp of low density aesthenospheric materials.

## EVOLUTION OF THE RIFT:

☐ *Pre-rift settings:*

* Most of southern N.M. was a cratonic back arc region during Laramide compressional event (65 Ma); only southwestern corner of state had a magmatic arc.
* Oligocene magmatism provided andesites and large volumes of rhyolitic ash flow tuff sheets from cauldron complexes.
* By about 30 ± 2 Ma the dominant, stable stress field had become one of extension.

■ *Early extension and volcanism (30-18 Ma):*

* Extension may have begun with a postulated rapid increase in the dip of the subducting slab.
* "Basaltic andesite" overlies the tuffs extensively; these flows are associated with shields or cones and can range from mafic andesite to latite (K-rich) and are calc-alkaline (high $SiO_2$, with Ca, K, Na).

Heat source which generated these materials may be related to an earlier, perhaps subduction-related, event and not the rifting directly. High geotherms made the lithosphere thin and weak, and onset of rifting may have provided the magma access to the surface.

* Broad, shallow basin formation from early ~30% NE-SW extension provided sediments that are interbedded with the volcanics. Closely-spaced low-angle faults are now observed in many mountain ranges (e.g., Organ Mts.) but are cross-cut by later high angle faults. Low-angle faults may have been originally high-angle or listric faults that were rotated. Extensional style and volcanism of this event is close to that of a similar era B&R phase.

☐ *Mid-Miocene magma gap (18-10 Ma):*

* Allows cooling and partial stabilization of lithophere as crustal extension slows.

■ *Late phase extension and volcanism (10-3 Ma):*

* 5-20% E-W extension was characterized by widely-spaced high-angle faulting resulting in uplifted narrow but deep horsts, grabens and tilted blocks.
* Volcanism changes to alkali-olivine and "true" basalts and continues until 0.18 Ma, although only small volumes were erupted in the southern rift.

OLSEN et al, 1987

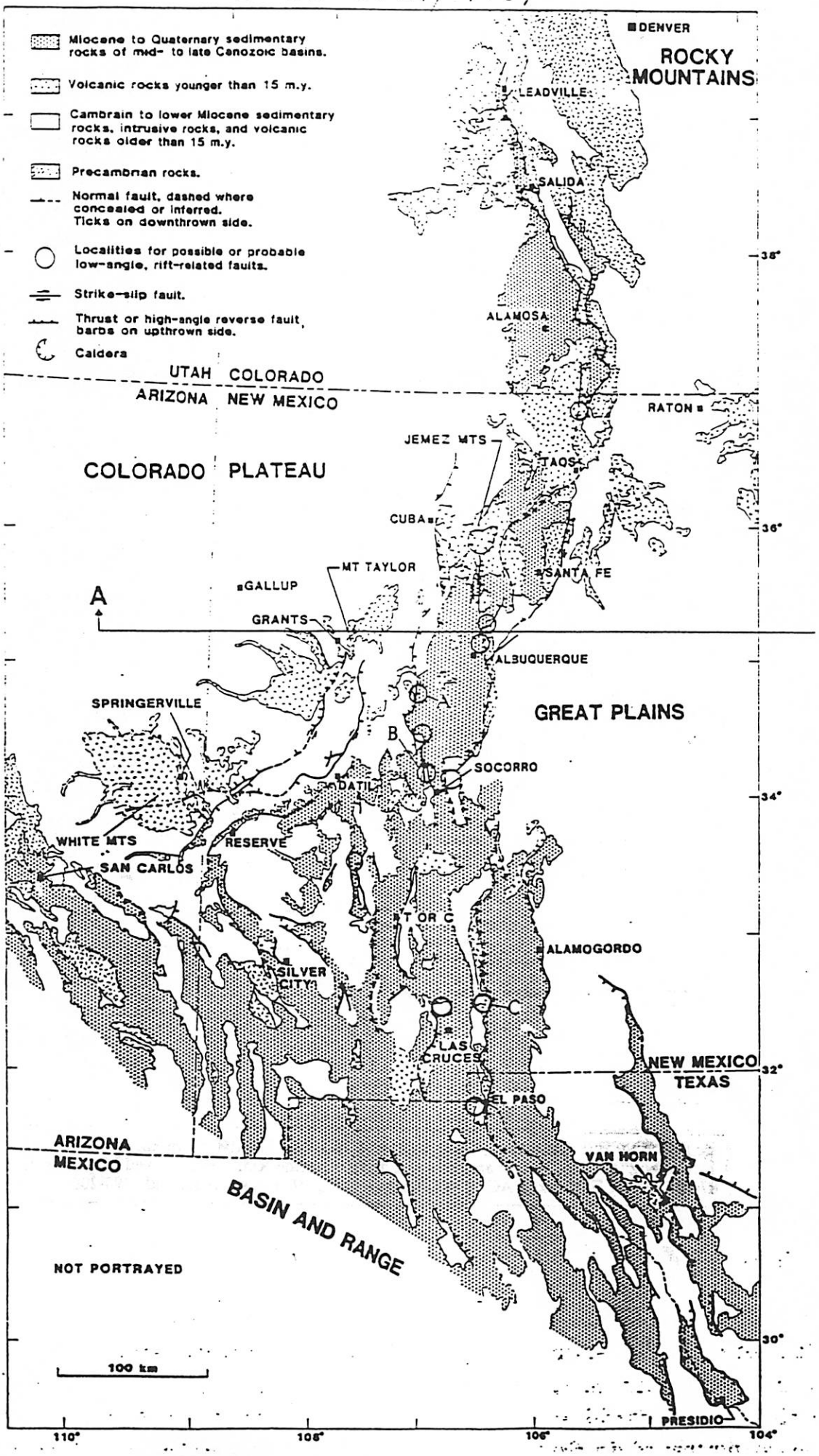

JJ3

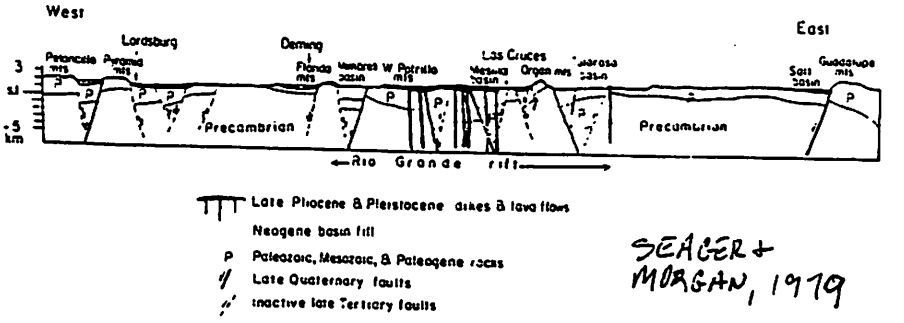


SEAGER + MORGAN, 1979

Fig. 7. Hypothetical cross-section through southern Rio Grande rift.

MORGAN et al., 1986

SEAGER + MORGAN, 1979

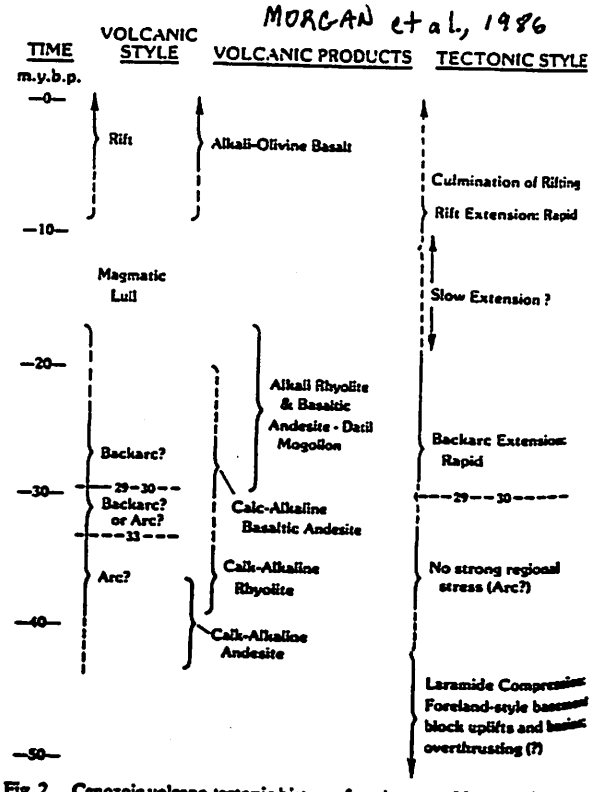


Fig. 2. Cenozoic volcano-tectonic history of southwestern New Mexico based on geologic data.

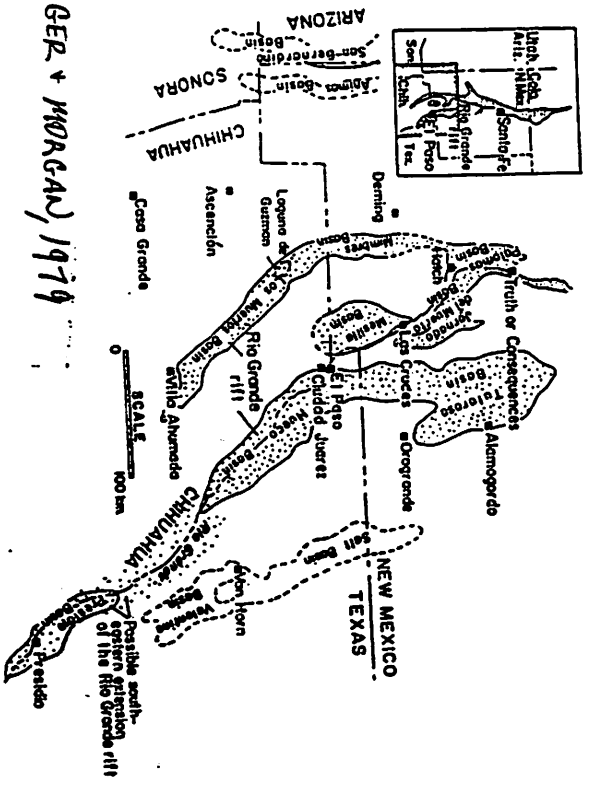


REFERENCES: Olsen et al., Tectonophysics, 143, 119-139, 1987; Morgan et al., JGR, 91, 6263-6276, 1986; Seager and Morgan, in Rio Grande Rift: Tectonics and Magmatism, 87-106, ed., R.E. Riecker, AGU, Washington, D.C., 1979; Cook et al., ibid., 195-208.

# The White Sands of New Mexico: Largest Gypsum Dune Field on Earth!

Your Helpful Hosts: Erik Asphaug and Jennifer Grier

Visitor Center Guide

Created millions of years ago by downfaulting of a huge block of the earth's crust, the Tularosa Basin is surrounded by mountains and highlands. In these mountains, including the forested Sacramentos to the east and the rugged San Andres to the west, are massive layers of gypsum rock.

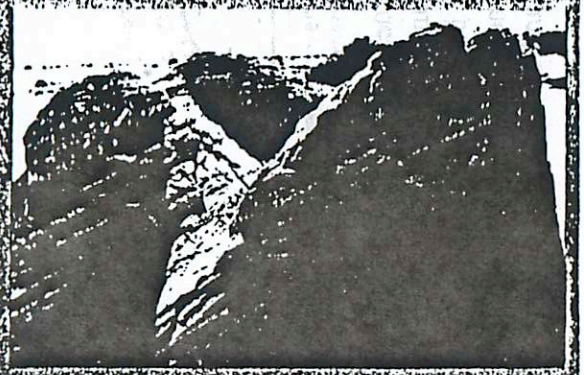

For centuries, waters collecting from seasonal rains and melting snows in these high ranges have eroded the gypsum deposits. The dissolved gypsum is carried into Lake Lucero, the lowest part of the basin. There the warm sun and dry winds prevalent much of the year evaporate the watery solvent, leaving gypsum crystals encrusted on lake bed.

The arid southwest wind persistently scours the bed of Lake Lucero and the alkali flats to the north. Weathering disintegrates the gypsum crystals into sand-size pulverulent grains which are swept by the wind and added to nearby embryonic sand dunes. As each dune grows and moves farther from the lake and flats, new ones form rank after rank in a seemingly endless procession.

From C.L. Herrick's 1900 description of the region (J.Geol. 8:112-128)...highly recommended....

Standing upon a jutting eminence of the San Andreas and turning eastward one looks out upon a scene difficult to parallel. At one's feet is an enormous plain, apparently as level as a floor, over forty miles wide and extending as far as eye can reach to north and south. On the southern horizon rise the Jarillas Mountains which only partially interrupt the plain, while to the northeast are the snow-capped peaks of the Sierra Blanca. Northward the plain is narrowed by the eastward intrusion of the Oscuro range while it is possible to make out the dark area of basalt which covers that part of the plain to the east and southeast of that range. This is the widely-know "*mal pais*" of Socorro county which has proven such an effectual barrier to communication between the Rio Grande valley and the growing region of White Oaks. South of the *mal pais* is a great white sea on which one can fancy the glint of white-caps. Such a body of water being out of the question the uninstructed observer would surely think himself the victim of a mirage but we recognize in the snowy area the famous white sands. Curious and conflicting stories are current respecting the area but the truth is not less interesting.

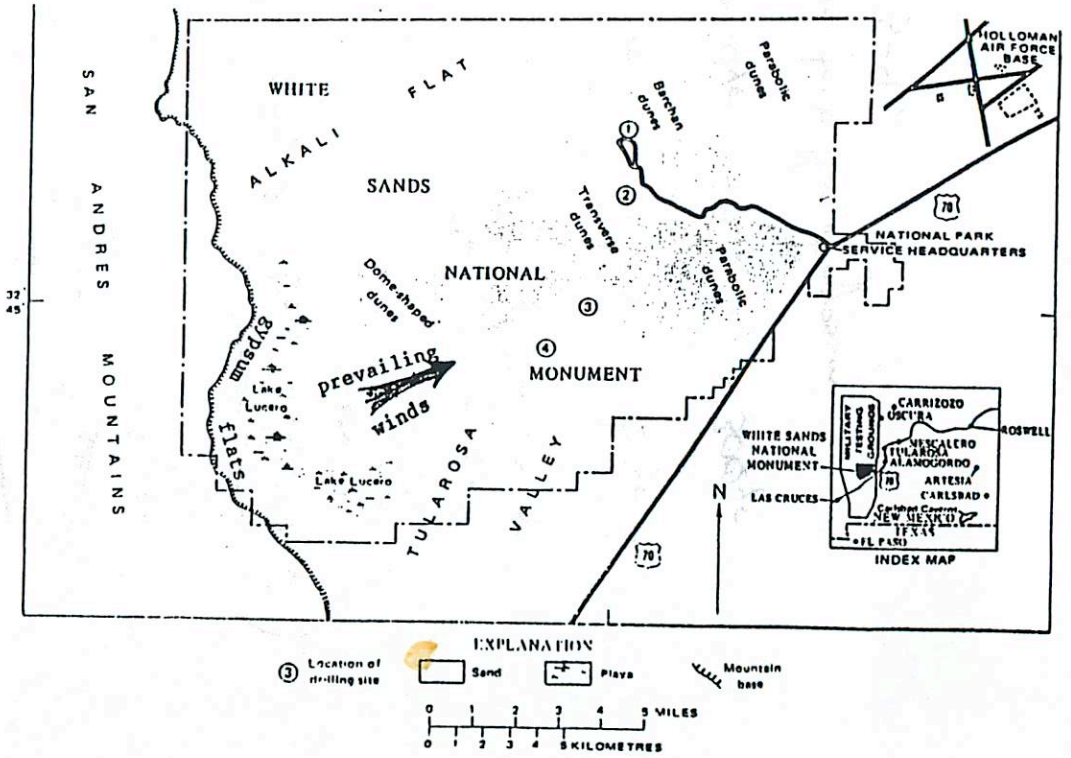

# Aeolean Processes in the Tularosa Basin

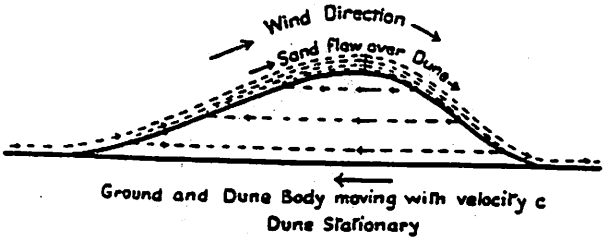


The migration rate of a dune is dependent on the mass transport rate at the crest, the transport rate at the trough, the dune height, and the bulk density. If the dune has a slip face, then the sand is "trapped" in the dune, and the transport rate of sand in the trough is zero.

$$c_r = \frac{q_c - q_t}{h\gamma}$$

$q_c$ = mass flux at crest
$q_t$ = mass flux at trough
$h$ = bedform height
$\gamma$ = bulk dune density

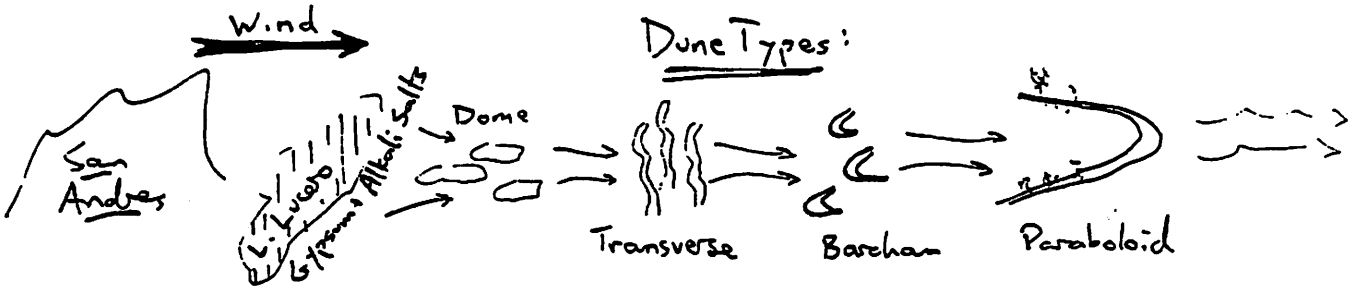


SE ( Plentiful Sand, Strong Wind, Sparse Vegetation ) —erosion of grains, dispersion of wind→ ( Scarce Sand, Less Constant Wind, Vegetation ) NW

| | | | |
|---|---|---|---|
| Dune Wavelength: | $\lambda \sim 150m$ | $\sim 150m$ | $\sim 1km$ (wide troughs) |
| Migration Rates: | $c_r \sim 10^m/_{yr}$ | $\sim 5^m/_{yr}$ | $\sim 3^m/_{yr}$ |
| Timescale $\tau = \frac{\lambda}{c_r}$ | $\sim 10yr$ | $\sim 50yr$ | $\sim 300yr$ |

Dunefield Depth: ~30m to bottom of gypsum
Dune height: $h \sim 3\text{-}9m$

# The Physics of Blown Sand
(after Bagnold)

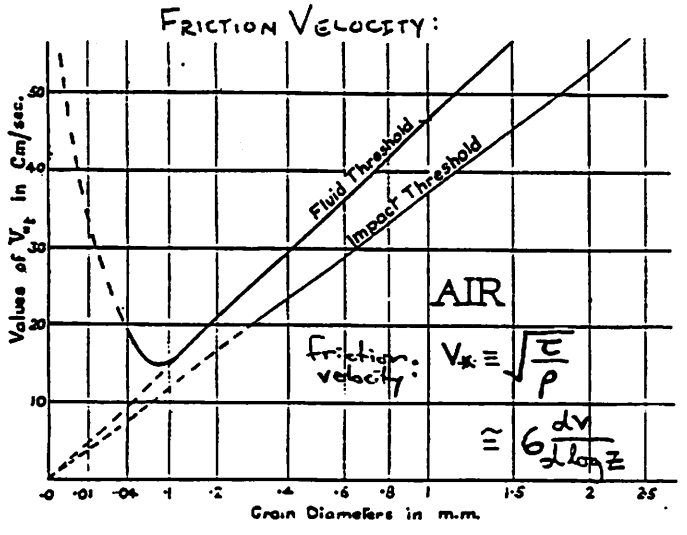


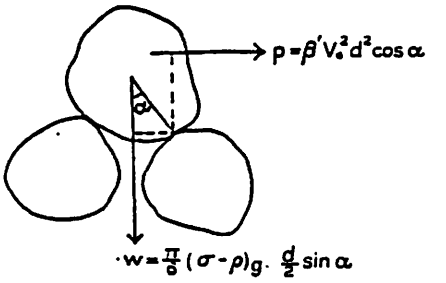


Threshold of Movement

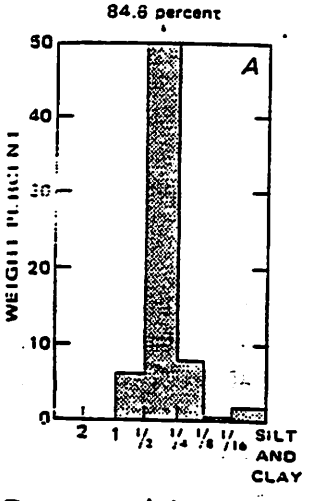


Dune sand is well-sorted.

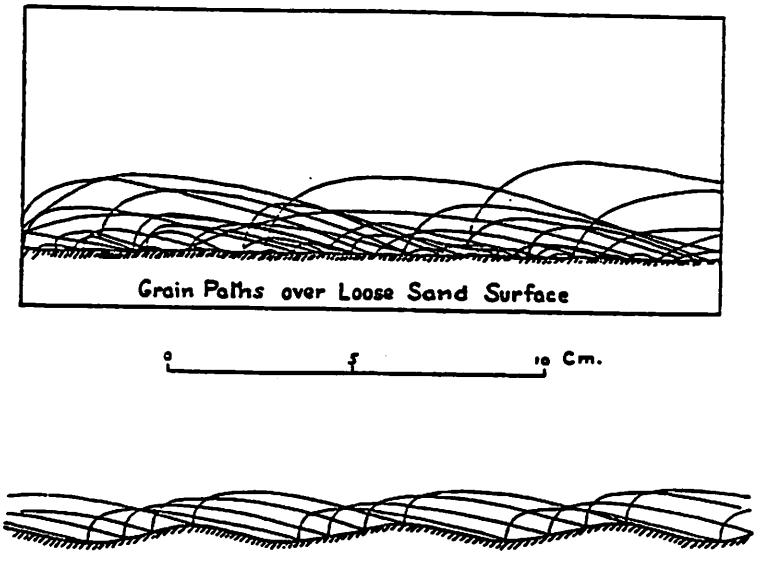


FIG. 49.—COINCIDENCE OF RIPPLE WAVELENGTH AND RANGE OF CHARACTERISTIC PATH OF GRAIN

For ⊕, ♂ and ♀:

| | Earth | Mars | Venus |
|---|---|---|---|
| Saltation Grain (microns) | 75–150 | 115 | 75 |
| Saltation Threshold (m/s) | 0.4 | 4.0 | .05 |
| Saltation Length (meters) | 0.2 | 42 | 0.3 |
| Impact Speed (m/s) | 1.6 m/s | 50 m/s | <10 cm/s |
| Grain Composition | Quartz (Gypsum, Clays, etc.) | Basalt? Clays? | ?? |

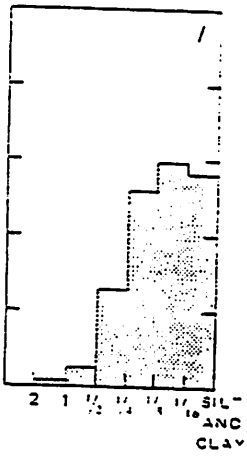


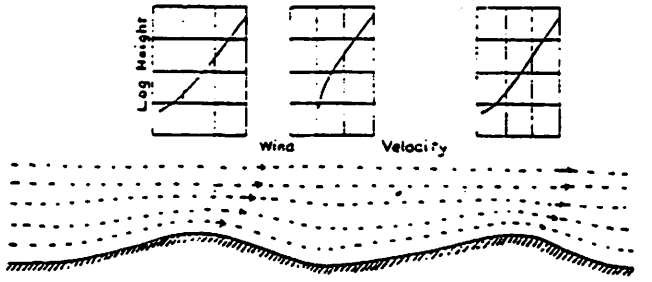


FIG. 50.—LOCAL DISTRIBUTION OF WIND VELOCITY OVER RIPPLES

Particles are poorly sorted in a dune trough: deposition from suspension

Dune Origin and Movement

The Tularosa Basin, which contains the White Sands National Monument, is bordered by the San Andreas Mountains to the west and the Sacramento Mountains to the east. These mountains contain thick layers of sedimentary rock (mostly shale and limestone). Gypsum, the single constituent of the dunes, is soluable in water. It is easily erroded away by rainfall from the limestone and carried to the lowest part of the basin, Lake Lucero. Since there is no outlet from the basin for the water in which the gypsum is dissolved, it collects here. Lake Lucero is a playa, usually dry most of the year. As the puddles of water evaporate, the gypsum forms a crust of selenite crystals on the lake bed. These crystals are very soft and easily broken and erroded down in size until they can be carried by the wind (saltated), and become sand.

The selenite sand is moved by strong, unidirectional winds. But even strong winds cannot lift sand more than a few feet off of the ground, on average. When the sand falls back down and impacts the sand beneath it, more sand is lofted up for the wind to carry. This jumping movement is saltation. The sand travels up the windward side of a dune, to the crest and over it, where sand begins to pile up. When the slope of this pile on the leeward side of the dune reaches approximately 34 degrees, sand slumping occurs. The four types of dunes at White Sands National Monument are Dome dunes (baby dunes), Transverse dunes, Barchan dunes, and Parabolic dunes.

## The following interesting questions come to mind:

1. What factors favor the establishment and survival of ecosystems in the dune troughs?
2. What determines the SW - NE extent of the White Sands? How does this relate to the dune morphology here?
3. Explain the existence of larger dune structures on Earth
4. What about dunes on Mars? What are they made of? How can they be so extensive?

# Carrizozo Lava Flow

Mark T Lemmon

Vital Statistics

Aliases: The Valley of Fires Lava Flow, or the Malpais.
Age: Quaternary, 1000-1500 years old.
Type: Pahoehoe flow, with three small cinder cones at the north end. Alkalic-tholeiitic basalts
Length: 75 km Width: 1-5 km Depth: 15-20 m
Area: 330 $km^2$ Volume: 4.2 $km^3$
Morphology:

Compound, tube fed, pahoehoe flow field
Highly vesicular, ropy flow surfaces with a glassy crust, tumuli (pressure domes), and collapse structures
No patches of a'a
Low slope - follows ancient stream bed
Signs of a vent (radiating flow patterns, cinder cones, lava shields, lava ponds) are found only near Little Black Peak

The problem presented by this otherwise typical pahoehoe flow is to determine why it is so long. The solution will allow a more informed interpretation of remote sensing data from other planets. What can make a long lava flow? [This is predominantly based on Keszthelyi & Pieri, 1992.] First, topography; but the slope of the Tularosa Basin floor is small. Second, rheology. However, based on chemical analysis of samples, the lava probably has higher viscosity than much shorter Hawaiian Pahoehoe flows. The Bingham yield strength is thought to be similar to lavas from Kilauea. There is no evidence of a high eruption temperature or of high water content, which could lower the viscosity. Finally, the eruption style could contribute to a long flow. The morphology indicates a point source in the north, as opposed to a long fissure vent. Empirical correlations with Hawaiian lava flows indicate an extremely high flow rate would produce a long flow (~1000 $m^3/s$ to get 75 km in length). However, pahoehoe is not observed with flow rates over 15 $m^3/s$. The lava becomes a'a due to the higher strain rate.

Keszthelyi & Pieri (1992) compare the flow to a particular Hawaiian lava flow (episode 48 of the 1983-present Pu'u O'o Kupaianaha flow). The Hawaiian flow had a flow rate of 5 $m^3/s$, and a length of 11 km. The flow was nearly continuous, allowing lava tubes to remain open and transport material away from the source. Thus, a long duration, continuous lava flow may be very long without requiring low viscosity or a high effusion rate.

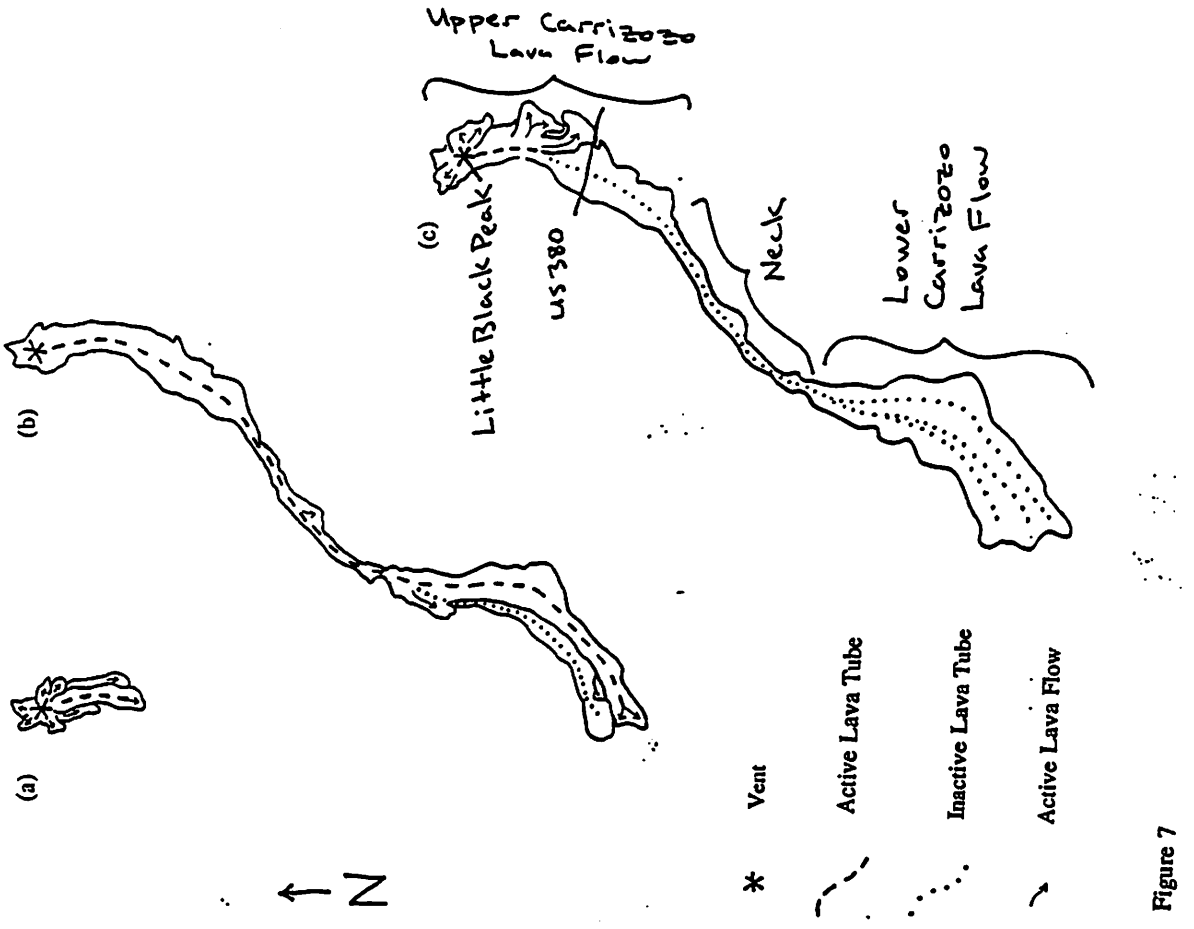


Figure 7

Figure 7 (Keszthelyi & Pieri, 1992): Possible emplacement history of the Carrizozo Flow Field based on episode 48 of the Pu'u O'o - Kupaianaha Flow Field. (a) The initial eruption was probably centered around the present location of Little Black Peak. Lava flows may have attempted to advance in all directions from the source, but found motion down the shallow slope preferable. (b) For some length of time, a large, stable tube system developed through the narrow "neck" region of the flow field. This tube fed a series sub-parallel, abutting flows to the south. (c) At some later point in time, this tube system broke down (possibly due to a longer pause in the eruption) and further flows built up around Little Black Peak, producing the topographic swell and radiating flow patterns observed in the present flow surface.

## References

Keszthelyi, L.P., and Pieri, D.C., 1992. Emplacement of the 75 km Long Carrizozo Lava Flow Field, South Central New Mexico. *Journal of Volcanology and Geothermal Research*, submitted.

Malin, M., 1980. Lengths of Hawaiian Lava Flows. *Geology* 8, pp.306-308.

Smith, C.T., 1964. Geology of the Little Black Peak Quadrangle and Lincoln, Counties, New Mexico. *New Mexico Geological Society 15th Field Conference*, pp.92-99.

Ulvag, C., and Thompson, III, S., 1964. Roadlog from Carrizozo to Malpais. *New Mexico Geological Society 15th Field Conference*, p.22.

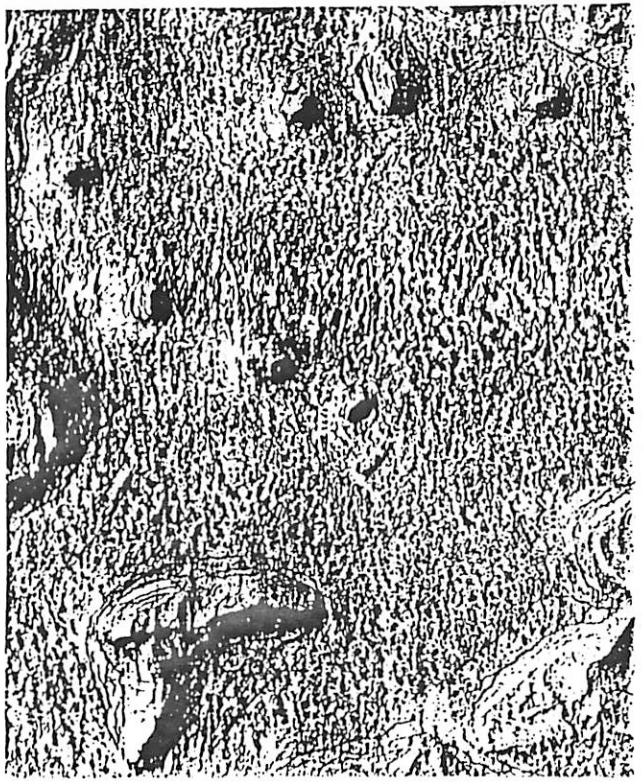

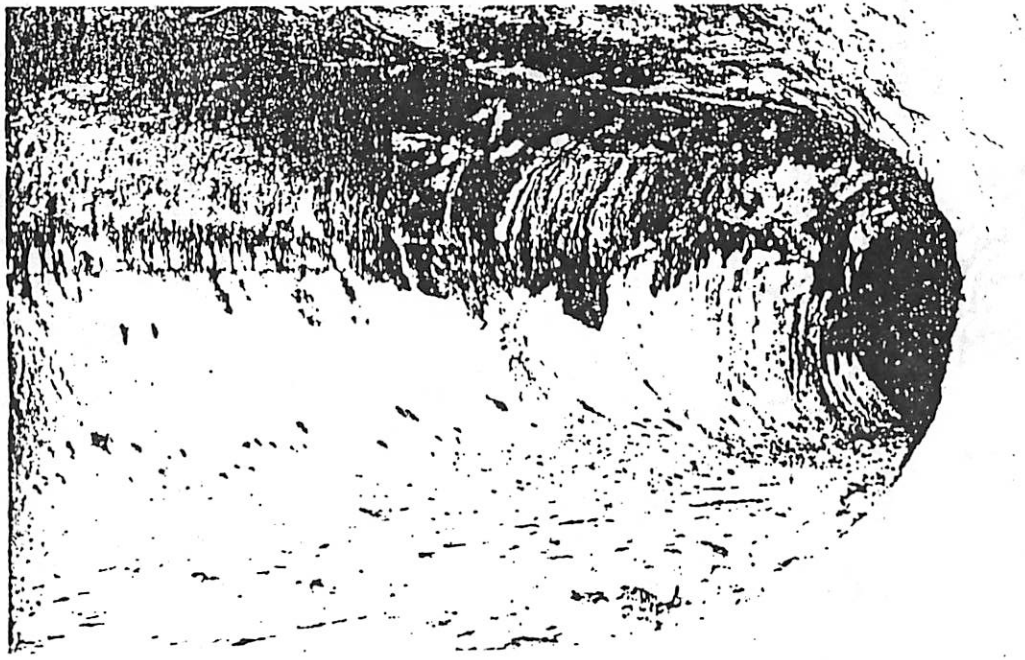

*Fig. 10* Valentine Cave, Lava Beds National Monument, California. A typical lava tube, of circular cross section, formed in olivine basalt. A flow line is seen on the opposite wall and a partial filling remains solidified as the floor. Tube height is about 2 m. (Photography by National Park Service, 1966.)

Fig. B
collepsed pits
(Bandera)

Fig. A

Fig. D
Lunar tubes

Fig. C
terrestrial tubes
(Bandera)

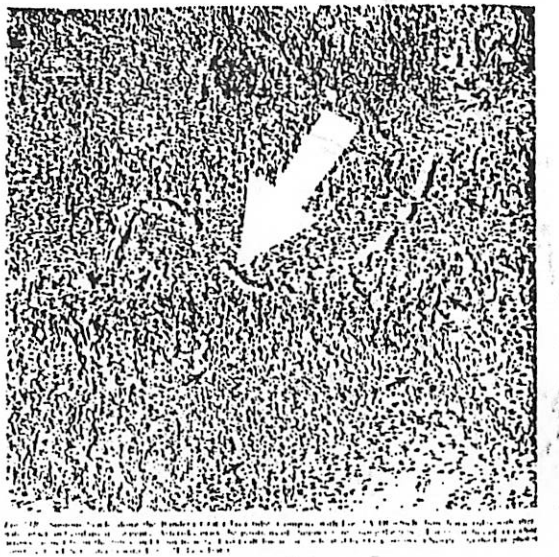

page 1
G. KOMATSU

page 2.
G. KOMATSU

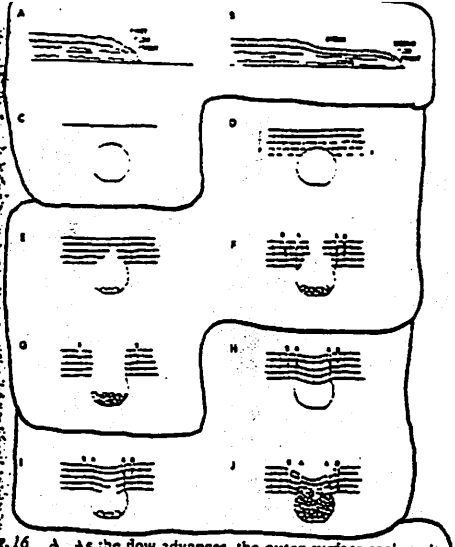

*Fig. 16* A. As the flow advances, the outer surface cools and solidifies, while the interior portions remain molten and fluid.

B. Hydrostatic pressure forces the molten interior against the immobile crust at the flow front, forming new flow units and draining lava from the interior.

C. Evacuation of lava creates a mobile cylinder of lava shearing a contact with the surrounding, more viscous lavas.

D. Differential cooling generates vertical joints which intersect the horizontal planes formed by laminar flow within the massive lava flow.

E. Joint cracks moving from the surface downward reach the upper surface of the tube and when contraction in the horizontal direction is sufficient, blocks begin to spall from the roof of the tube. Some plastic deformation may also occur along the upper interior surface of the tube. Shear planes may develop along the lower interior surface in areas in which heat dissipation has occurred to a lesser degree and where the rock may still be plastic.

F. Primary (A) and secondary (B) tensile fractures form in the roof arch and begin to outline a peripheral failure of the tube.

G. Final failure occurs along primary tensile fractures and the cycle is complete. The process may be assisted by seismic activity of a volcanic nature.

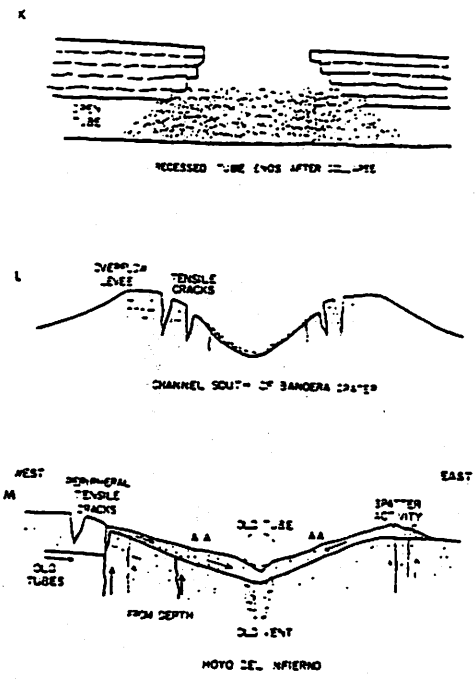


H. OR: Plastic deflection of the roof area results in deformation of the tube cross section.

I. Spalling then occurs.

J. The tube is filled with rubble and tilted slabs of basalt. In some instances this rubble fills the collapse pit to a point above the original roof line and the lava tube is made inaccessible.

K. Cave-like recesses found at the ends of many collapse pits along the lava tubes.

L. Diagrammatic cross-section of the channel on the Bandera Crater lava tube S of the crater. (See also Fig. 17.)

M. Diagrammatic cross-section of the Hoyo del Infierno subsidence pit. The interior of the pit is now largely covered with aa lava extruded through fissure vents and tensile cracks onto a surface of tilted pahoehoe slabs. (See also Figs. 25A and B.)

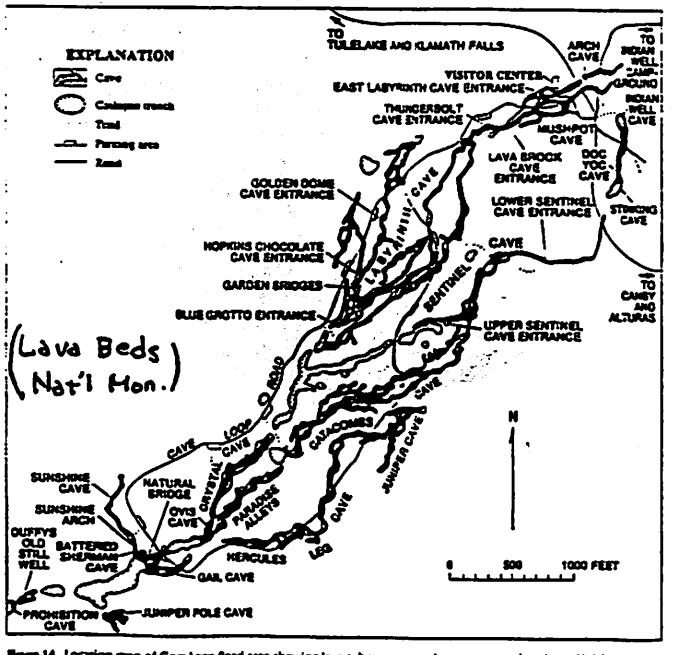


Figure 14. Location map of Cave Loop flood area showing lava-tube systems and cave entrance locations. Unlabeled roads in upper-right corner of map are shown in detail on map 1, pl. 1.



F:g. H

F:g. E

F:g. G

F:g. F

* Vent

Active Lava Tube

Inactive Lava Tube

Active Lava Flow

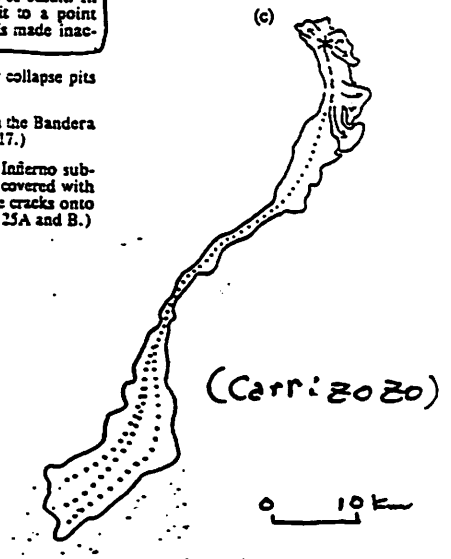


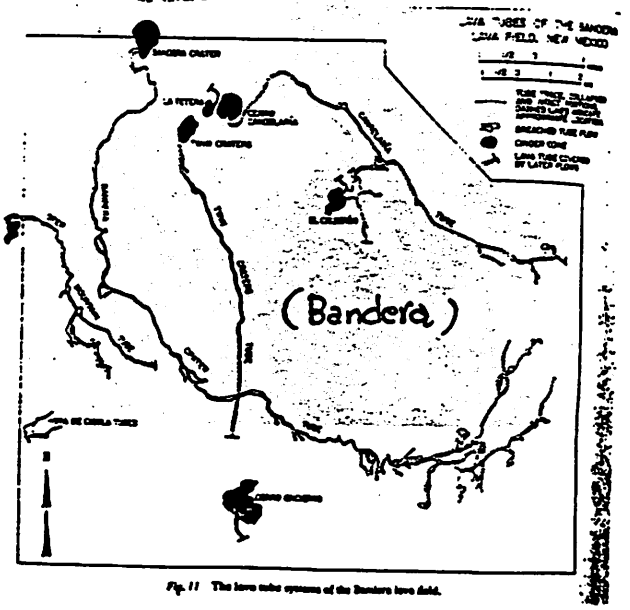


*Fig. 11* The lava tube systems of the Bandera lava field.

# Special Report:

# Comet Swift-Tuttle

# Impact of Comet Swift-Tuttle by Erich Karkoschka

In the early morning hours of Wednesday, August 14, 2126, comet Swift-Tuttle will impact in south-eastern Arizona/south-western New Mexico at a speed of 60 km/s, coming from the north-east at about 45° angle and producing an impact crater of 100—200 km diameter, or the comet will be at least in our vicinity (that means within 100 million km).

Comet Swift-Tuttle is the only known comet or asteroid which can collide with the earth in the near future. It is probably one of the largest known comets (estimates put it at 10—20 km diameter) and larger than all earth-approaching asteroids.

**History:** Comet Swift-Tuttle is also called The Great Comet of 1862. Observations in 1862 indicated an orbital period near 120 years and thus a return between 1979 and 1983. The Italian astronomer Giovanni Schiaparelli noted that its orbit is identical to the orbit of the Perseid meteor shower, making the connection between cometary debris and meteor showers. In 1980 and 1981, the Perseids were very active, but the comet was not seen. Brian Marsden noted that Swift-Tuttle may be identical to Kegler's comet of 1737 and predicted a perihelion date next week (late November 1992). Again, this was supported by increasing Perseid activity during the last years, peaking to possibly 8000 meteors/hour in 1992 compared to typical 100/hour in normal years.

**Present:** On September 26, 1992 (after our first field trip meeting), Japanese Tsuruhiko Kiuchi recovered comet Swift-Tuttle. The comet is brightest during the second half of November and is then visible by naked eye. Because of its low surface brightness it is best seen away from city lights such as the Chiricahua Mountains and the Rio Grande Swift.

**Future:** Swift-Tuttle will be at perihelion on December 12, 1992 and it will cross the ecliptic on December 31, only 130 000 km inside of earth's orbit. It should return to this point in late July, 2126, two weeks before the earth will be there. However, outbursts of the comet can change the orbit by more than 100 000 km and can also change the arrival time by several weeks. This time, it also came two weeks late. Non-gravitational forces occur usually near perihelion. Therefore, accurate observations in 1993 and the following years may lead to a much more reliable arrival time. The thrust by these forces during one perihelion passage is about five orders of magnitude greater that the thrust of a Saturn V rocket.

Given that the arrival time of the comet must be within a four minute long time interval in order to hit the earth, the probability of impact is roughly one part in 10 000 to one part in one million. The probability of impact in south-eastern Arizona/south-western New Mexico is three orders of magnitude smaller. A chance of one part in one million in 100 years is quite consistent with estimates that large impacts and mass extinctions occur approximately once every 100 million years. Comet Swift-Tuttle gives us another view of large impacts in history and future.